4 Energy-Efficient Signaling Design and Resource Management

The fundamental issues of energy-efficient design have been discussed in Chapter 2, from the perspectives of information theory and optimization theory. Those ideas and methods mainly focus on single-cell network scenarios where energy-efficient design can be coordinated at a single base station (BS). These approaches merely aim at link-level energy efficiency (EE) by optimizing radio resource allocation. However, the operation of a BS contributes to 60–80% of the overall network energy consumption and is the main source of energy usage. Therefore, energy-saving of BSs plays an important role in green cellular networks.

Beyond energy-efficient radio resource optimization at the link level, in this chapter we discuss green communication approaches from the perspective of network architecture. Currently, most cellular networks consist of homogenous BSs, which can cover an area with a radius from 100m to 10km. The energy consumption of these macro-cell BSs is usually very high since high-transmit power is required to maintain large network coverage. Moreover, most of them are equipped with cooling systems, consuming a large amount of energy. Thus, the dynamic management of the operation status of BSs, i.e., adaptive sleep control, is an essential issue for saving network energy consumption.

On the other hand, a heterogenous cellular structure with different kinds of densely deployed BSs will be adopted by future cellular networks. Such heterogenous networks (HetNets) with small-cell BSs can greatly reduce the energy consumption of both network and user devices. First, the transmit power of BSs can be considerably reduced due to the smaller network coverage size. Furthermore, compared with macro BSs, the operation of small-cell BSs is much more energy efficient without the cooling system. The HetNet architecture can also reduce the energy consumption of mobile devices due to the shortened distance between user devices and serving BSs.

According to the radio access technology (RAT) used, HetNets can be classified into two types: single-RAT HetNet and multi-RAT HetNet. Single-RAT HetNet consists of BSs with the same radio access protocol, such as LTE BSs. On the other hand, multi-RAT HetNet consists of BSs with different radio access protocols, e.g., LTE BSs and WiFi access points. A single-RAT HetNet has a much easier network control, whereas intercell interference coordination is much more complicated due to frequency reuse among cells. On the other hand, the network control of multi-RAT HetNet is somewhat difficult due to various types of access points. However, intercell interference coordination could be much easier, since different RATs may transmit at different frequency bands.

https://doi.org/10.1017/9781108277389.005 Published online by Cambridge University Press

In the rest of this chapter, we will discuss green communication techniques from the network-layer perspective. In particular, we will introduce several sleep control and cell zooming strategies for BSs in Section 4.1. In Section 4.2, we will present a joint downlink and uplink energy-efficient resource allocation algorithm. Sections 4.3 and 4.4 discuss the energy-efficient design issues in homogenous and heterogeneous networks, respectively.

4.1 Sleeping Strategy and Cell Zooming

4.1.1 Dynamic Base Station Sleep Control

Cellular network operators have been continuously seeking ways to increase EE in all components of cellular networks, including mobile devices, BSs, and core (backhaul) networks. There has been a tremendous amount of work on mobile device EE with the objective of prolonging battery life. Similarly, green operation of the Internet has been considered, and some of the techniques can be extended to the cellular backhaul networks. However, as mentioned before, the key source of energy usage in cellular networks is the operation of BS equipment, which contributes to almost 60–80% of total energy consumption. Therefore, the energy-efficient operation of cellular BSs is the key challenge to implementing the so-called green cellular network.

The traditional network architecture is designed based on the assumption that user requests may happen anytime and anyplace. Therefore, to guarantee cell coverage and provide appropriate services for potential requests, most existing cellular networks have been designed to keep the transmit power always on, which is clearly not energy efficient, since the user requests occur only sometimes and somewhere in practice.

Energy-efficient design of BSs has been considered in all stages of cellular networks, including hardware design and manufacture, deployment, and operation. However, there is also room for significant improvement in cellular operation. In fact, the BS consumes more than 90% of its peak energy while experiencing little or even no activity. As a result, turning off some radio transceivers at BSs with low traffic load can save some energy consumption but is still not sufficient for green cellular operation. To obtain significant energy savings, BS sleeping, a carefully coordinated dynamic approach, has been developed and involves the operation of shutting entire BSs and transferring the corresponding load to neighboring cells during periods of low utilization.

BS sleeping has attracted more and more attention in recent years [1–3], and there have been many ways to facilitate its implementation. Early works mainly focused on static BS sleep according to deterministic traffic patterns over time, without considering randomness and spatial variation. However, for the path-loss-dominant cellular network, a dynamic clustering algorithm considering BS collaboration is more effective. A common principle is to dynamically adjust the work modes (active or sleeping) of BSs according to the traffic variation with respect to certain blocking probability requirements. Moreover, BSs should hold their current working modes for at least a given interval to prevent frequent mode switching.

https://doi.org/10.1017/9781108277389.005 Published online by Cambridge University Press

The most challenging issue of dynamic BS sleep control is to maintain the cell coverage. Among all methods, the most direct one is to increase the coverage area of the nearby BSs. There are two alternative ways to realize this: increasing the transmission power or utilizing lower-frequency bands with better penetration capacity under the same transmission power constraint. Besides, appropriate design of multi-hop relay and coordinated multipoint transmission will also be clearly useful to ensure that the dynamic shutting down of BSs will not leave any coverage hole. More detailed granularity of control and more differentiated heterogeneous cell sizes should also be carefully designed.

4.1.2 Cell Zooming for Green Cellular Networks

Different from the dynamic BS sleep control in the previous sections, in this section, we introduce a dynamic cell zooming strategy to facilitate the implementation of green cellular networks [4].

The cell sizes and the transmit power on the control channel of traditional cellular BSs are usually fixed. The cell size of a BS can be regarded as the area where the power of the received control signal from the BS is above a given threshold. The cell size of each BS is usually predetermined according to the estimated traffic load when the network is established. In the past voice traffic dominated the cellular traffic load, and thus fixed cell size could achieve satisfactory network performance with simple network management. However, as wireless data traffic has grown very rapidly in the past few years, traffic loads are significantly dynamic among different cells. Both spatial and temporal traffic fluctuations can be observed. As discussed before, dynamic BS sleep control can be applied to save network energy consumption. For example, in the nighttime, some BSs located in office areas can be switched off due to the relatively light traffic load. In this situation, the cell size of each BS should be adaptively adjusted according to the traffic dynamics. This phenomenon is known as cell zooming, which can not only balance the traffic load but also reduce network energy consumption.

There have been many ways to facilitate the implementation of cell zooming. The simplest one is to adjust the physical parameters of BSs, such as transmit power control and antenna tilt adaption. Increasing the transmit power can zoom out the cell size, while adjusting the antenna tilt can change the coverage area. Another effective means is BS cooperation where neighboring BSs can utilize the coordinated multipoint (CoMP) transmission to form a cluster. Besides these two methods, leveraging the BS relaying technique or D2D communications is also an effective method to realize the cell zooming [5, 6].

Figure 4.1 shows an example of cell zooming for green cellular networks in which the BS in the center cell decides to sleep due to the low traffic load. In this situation, the nearby BS will trigger the cell zooming operation. Among them, BS1 and BS4 increase their transmit powers to enlarge cell coverage, BS2 and BS3 leverage the relay technique to cover some areas of the sleeping cell, while BS5 and BS6 utilize the CoMP transmission to expand the network coverage.

https://doi.org/10.1017/9781108277389.005 Published online by Cambridge University Press

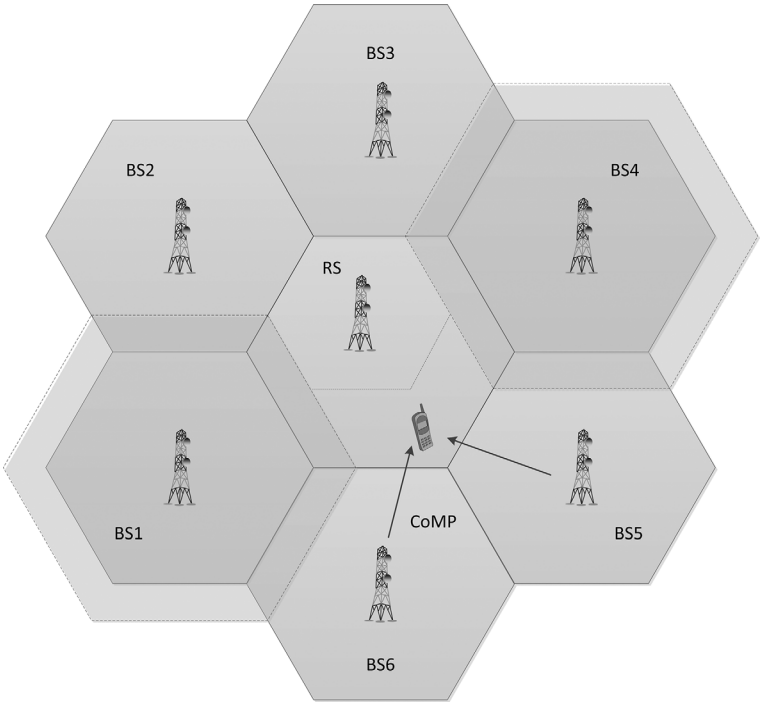

Figure 4.1 An illustration of cell zooming for green cellular networks.

4.1.3 Soft-Defined Network Architecture for Green Cellular Networks

In traditional cellular systems, the physical infrastructure consists of geographically distributed hardware subsystems including the BSs. These subsystems are often dedicated for specific tasks and present network functions together by communicating with each other via predefined network protocols. Although traditional cellular systems have sufficient capabilities to serve traffic with traditional moderate QoS requirements, there are several severe problems that must be addressed in order to reach the demand of next-generation communications.

- Flexibility. The proprietary subsystems and interfacing protocols make it hard to update the traditional cellular system's functions or add services. It would be energy-consuming for the widely-deployed subsystems.
- Efficiency. The distributed system layout prohibits cooperation technologies like CoMP. As a result, the network performance cannot be improved via intercell and inter-network cooperation. Dynamic BS sleeping control and cell zooming cannot be implemented either.
- Resource utilization. Geographically distributed subsystems rely on local physical resources to function. Thus, resources must be overprovisioned for peak load, leading to a low resource utilization efficiency.

https://doi.org/10.1017/9781108277389.005 Published online by Cambridge University Press

Thus, it is proposed that 5G networks should be constructed with centralized physical resource placement and become increasingly software-defined. In general, the emerging cellular system architectures should be developed from the following three aspects [7, 8].

- Separation of the air interface. Aiming at flexible and efficient control of small cells for throughput boosting, energy-saving, and BS sleeping, the separation of signaling and data should be featured in the new air interface architecture of cellular networks. Therefore, the data traffic service is relative to demand, whereas the control plane is always "on," to guarantee basic coverage.
- Base station functions virtualization. By providing programmable BS functions and reconfigurable radio elements, flexible and efficient signal processing can be implemented to reconstruct the frame components from the control and traffic layers of the air interface. In this way, control-traffic-decoupled air interface can be realized.
- Soft-defined networking. By separating the control and data planes, the SDN architecture enables centralized optimization of data transmission. In addition, the control-data separation in SDN can be extended to wireless access layer by the control-traffic-decoupled air interface.

4.2 Joint Optimization of Uplink and Downlink Energy Efficiency

There are generally two different trends for energy-efficient design in cellular networks. One is energy-efficient design for downlink transmission, the other is energy-efficient design for uplink transmission. The former mainly saves power consumption of BSs from the perspective of cellular network operators, and the latter mainly saves power consumption of mobile devices from the perspective of users. Most previous studies have only focused on one aspect of energy-efficient design, either uplink [9–11] or downlink [11–15]. Those energy-efficient algorithms proposed in the existing literature may cause unbalance of uplink EE and downlink EE. In this section, we will present a framework to simultaneously optimize both EEs by joint downlink and uplink resource allocation.

To do so, we consider a cellular network with carrier aggregation (CA), which allows users to aggregate different sub-bands to achieve a larger data rate. We also consider a time division duplex (TDD) operation, which enables dynamic allocation of uplink and downlink resource to guarantee the performance of both BS and user devices. In a TDD CA system, the uplink to downlink resource ratio on each sub-band can be optimized. Existing literature has investigated this problem from the perspective of throughput enhancement and network load balance while the EE issue has not been studied yet [16–19].

In what follows, we will first briefly introduce the system model, and then formulate the EE optimization problem. Then, a joint uplink and downlink resource allocation

https://doi.org/10.1017/9781108277389.005 Published online by Cambridge University Press

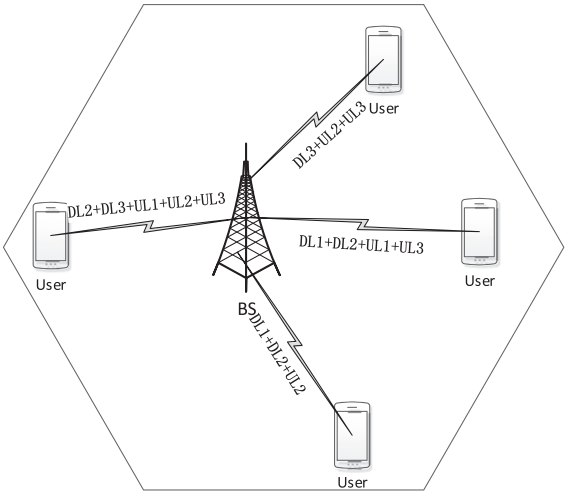

DL1: Downlink bandwidth from band 1. UL1: Uplink bandwidth from band 1.
DL2: Downlink bandwidth from band 2. UL2: Uplink bandwidth from band 2.
DL3: Downlink bandwidth from band 3. UL3: Uplink bandwidth from band 3.

Figure 4.2 The network model of the TDD CA system.

algorithm will be developed. Finally, numerical simulation results are provided to validate the effectiveness of the proposed algorithm.

4.2.1 System Model and Problem Formulation

As depicted in Fig. 4.2, we consider a TDD CA system with M users, $\mathcal{M} = \{1, 2, \cdots, M\}$, and N available sub-bands, $\mathcal{N} = \{1, 2, \cdots, N\}$. Each user can dynamically transmit on several sub-bands according to the user's channel power gains and data rate requirement. Moreover, the uplink to downlink resource ratio on each sub-band can also be dynamically chosen to balance the uplink and downlink performance. The channel between user m and the BS on the n-th sub-band follows the i.i.d. Rayleigh fading model, as

$$g_{m,n} = \Gamma_n h_{m,n} d_m^{-\alpha_n}. \tag{4.1}$$

In (4.1), d_m denotes the distance between user m and the BS, α_n is the path loss exponent of the sub-band n, Γ_n is the path loss constant of the sub-band n, and $h_{m,n}$ is the random variable reflecting the small-scale fading and the shadowing effect. We further assume that uplink and downlink transmissions have the same channel power gain due to the channel reciprocity of TDD.

To simplify our analysis, we only consider a single-cell TDD system where intercell interference can be ignored. Then, we can express the signal-to-noise ratio (SNR) for user m on sub-band n as

https://doi.org/10.1017/9781108277389.005 Published online by Cambridge University Press

$$\mathrm{SNR}_{m,n}^{x} = \frac{p_{m,n}^{x} g_{m,n}}{b_{m,n}^{x} N_0}, \forall m, n, \tag{4.2}$$

where x can be UL or DL (standing for uplink or downlink, respectively), N_0 is the power spectral density of the additive white Gaussian noise (AWGN), $p_{m,n}^{x} \geq 0$ denotes the transmit power allocated to user m on sub-band n, and $b_{m,n}^{x} \geq 0$ denotes the bandwidth allocation. According to the Shannon formulation, the transmit data rate for user m on sub-band n can be expressed as

$$R_{m,n}^{x} = b_{m,n}^{x} \log_2 \left(1 + SNR_{m,n}^{x}\right), x = 'UL' \text{ or } 'DL', \ \forall m, n. \tag{4.3}$$

Since we need to optimize the EE of both downlink and uplink, we shall calculate the overall data rate of both the BS and user devices. The overall transmitted data rate of the BS can be expressed as

$$R_0 = \sum_{n=1}^{N} \sum_{m=1}^{M} b_{m,n}^{\mathrm{DL}} \log_2 \left(1 + \frac{g_{m,n} p_{m,n}^{\mathrm{DL}}}{b_{m,n}^{\mathrm{DL}} N_0}\right), \tag{4.4}$$

and the transmitted data rate of user m can be expressed as

$$R_m = \sum_{n=1}^{N} b_{m,n}^{\mathrm{UL}} \log_2 \left(1 + \frac{g_{m,n} p_{m,n}^{\mathrm{UL}}}{b_{m,n}^{\mathrm{UL}} N_0}\right). \tag{4.5}$$

We shall also model the power consumption of the BS and user devices. The power consumption mainly includes three parts, which can be expressed as

$$P_0 = \sum_{n=1}^{N} \sum_{m=1}^{M} w_n p_{m,n}^{\mathrm{DL}} + P^{\mathrm{DL,I}} + \sum_{n=1}^{N} P_n^{\mathrm{DL,D}} \sum_{m=1}^{M} \left(b_{m,n}^{\mathrm{DL}} + b_{m,n}^{\mathrm{UL}}\right), \tag{4.6}$$

where the first item is the radio frequency (RF) power consumption (w_n denotes the inverse of the power amplifier efficiency on sub-band n), the second item is the fixed circuit power consumption, and the third item is the circuit power consumption related to the total occupied bandwidth ($P_n^{\mathrm{DL,D}}$ denotes the power consumption per unit bandwidth).

The total power consumption for user m can be modeled in a similar way as

$$P_m = \sum_{n=1}^{N} v_n p_{m,n}^{\mathrm{UL}} + P^{\mathrm{UL,I}} + \sum_{n=1}^{N} \left(b_{m,n}^{\mathrm{DL}} + b_{m,n}^{\mathrm{UL}}\right) P_n^{\mathrm{UL,D}}. \tag{4.7}$$

This power consumption also contains three parts, with v_n representing the inverse of the power amplifier efficiency at the user device, $P^{\mathrm{UL,I}}$ being the fixed circuit power consumption, and $P_n^{\mathrm{UL,D}}$ being the bandwidth-related power consumption.

Now we are ready to express the EEs for the downlink and the uplink as

$$\chi_0 = \frac{R_0}{P_0}, \tag{4.8}$$

https://doi.org/10.1017/9781108277389.005 Published online by Cambridge University Press

and

$$\chi_m = \frac{R_m}{P_m}, m = 1, 2, \cdots, M, \tag{4.9}$$

respectively.

The objective of this section is to develop a joint downlink and uplink resource allocation algorithm to maximize the EE of both the BS and user devices. Therefore, the optimization problem can be formulated as

$$\max_{\mathbf{P},\mathbf{B}} \sum_{m=0}^{M} \eta_m \chi_m, \tag{4.10a}$$

subject to

$$\sum_{n=1}^{N} p_{m,n}^{\mathrm{UL}} \le p_m^{\mathrm{UL,max}}, \forall m, \tag{4.10b}$$

$$\sum_{m=1}^{M}\sum_{n=1}^{N} p_{m,n}^{\mathrm{DL}} \le p^{\mathrm{DL,max}}, \tag{4.10c}$$

$$\sum_{m=1}^{M} \left(b_{m,n}^{\mathrm{DL}} + b_{m,n}^{\mathrm{UL}} \right) \le W_n, \forall n, \tag{4.10d}$$

$$\sum_{n=1}^{N} b_{m,n}^{\mathrm{UL}} \log_2 \left(1 + \frac{g_{m,n} p_{m,n}^{\mathrm{UL}}}{b_{m,n}^{\mathrm{UL}} N_0} \right) \ge R_m^{\mathrm{UL,min}}, \forall m, \tag{4.10e}$$

$$\sum_{n=1}^{N} b_{m,n}^{\mathrm{DL}} \log_2 \left(1 + \frac{g_{m,n} p_{m,n}^{\mathrm{DL}}}{b_{m,n}^{\mathrm{DL}} N_0} \right) \ge R_m^{\mathrm{DL,min}}, \forall m, \tag{4.10f}$$

$$b_{m,n}^{\mathrm{DL}} \ge 0,\ b_{m,n}^{\mathrm{UL}} \ge 0,\ p_{m,n}^{\mathrm{DL}} \ge 0,\ p_{m,n}^{\mathrm{UL}} \ge 0, \forall m, n. \tag{4.10g}$$

Here, η_0 is the weight value for downlink EE and η_m ($m \in \{1, 2, \cdots M\}$) is the weight value for uplink EE of user m. They are all predetermined by the network operator to characterize the relative importance of network energy consumption and user energy consumption. $\mathbf{P}_{M\times 2N} = [\ \mathbf{p}^{\mathrm{DL}}, \mathbf{p}^{\mathrm{UL}}\ ]$ and $\mathbf{B}_{M\times 2N} = [\ \mathbf{b}^{\mathrm{DL}}, \mathbf{b}^{\mathrm{UL}}\ ]$, where $\mathbf{p}^{\mathrm{DL}}$, $\mathbf{p}^{\mathrm{UL}}$, $\mathbf{b}^{\mathrm{DL}}$, and $\mathbf{b}^{\mathrm{UL}}$ are all $M \times N$ matrices collecting the elements of $p_{m,n}^{\mathrm{DL}}$, $p_{m,n}^{\mathrm{UL}}$, $b_{m,n}^{\mathrm{DL}}$, and $b_{m,n}^{\mathrm{UL}}$, respectively. The constraints in (4.10b) and (4.10c) restrict the maximum transmit power for each user and the BS, respectively. The constraint in (4.10d) indicates the total uplink and downlink bandwidth on each sub-band. The constraints in (4.10e) and (4.10f) guarantee the minimum uplink and downlink data rates for user m, respectively.

https://doi.org/10.1017/9781108277389.005 Published online by Cambridge University Press

4.2.2 Joint Uplink and Downlink Resource Allocation

The problem in (4.10a) is obviously a sum-of-ratios optimization problem, i.e., maximizing the summation of several fractional functions. As described in the Appendix in Chapter 2, this problem can be effectively solved by the sum-of-ratios algorithm by transforming it into an equivalent convex optimization problem, as shown in the following theorem.

THEOREM 4.1 *If* $(\mathbf{P}^*, \mathbf{B}^*)$ *is the optimal solution to* (4.10)*, then there exist* $\boldsymbol{u}^* = \left(u_0^*, u_1^*, \cdots, u_M^*\right)$ *and* $\boldsymbol{\beta}^* = \left(\beta_0^*, \beta_1^*, \cdots, \beta_M^*\right)$ *such that* $(\mathbf{P}^*, \mathbf{B}^*)$ *is a solution to the following problem under the constraints from* (4.10b) *to* (4.10g) *for* $\boldsymbol{u} = \boldsymbol{u}^*$ *and* $\boldsymbol{\beta} = \boldsymbol{\beta}^*$

$$\max_{\mathbf{P},\mathbf{B}} \sum_{m=0}^{M} u_m \left(\eta_m R_m - \beta_m P_m\right). \tag{4.11}$$

Moreover, $(\mathbf{P}^*, \mathbf{B}^*)$ *also satisfies the following system of equations for* $\boldsymbol{u} = \boldsymbol{u}^*$ *and* $\boldsymbol{\beta} = \boldsymbol{\beta}^*$*:*

$$u_m = \frac{1}{P_m}, m = 0, 1, \cdots, M, \tag{4.12}$$

$$\beta_m = \eta_m \chi_m, m = 0, 1, \cdots, M. \tag{4.13}$$

From the above theorem, the fractional objective function has been changed into a subtractive form as $\sum_{m=0}^{M} u_m \left(\eta_m R_m - \beta_m P_m\right)$. Thus, we can achieve the global optimal solution to the original problem by equivalently solving this problem. We now prove that the equivalent problem is jointly concave on $(\mathbf{P}, \mathbf{B})$.

Define $U\left(\mathbf{P}, \mathbf{B}\right) = \sum_{m=0}^{M} u_m \left(\eta_m R_m - \beta_m P_m\right)$ and $\mathbf{H}\left(U_{m,n}\left(\mathbf{P}, \mathbf{B}\right)\right)$ as the Hessian of $U\left(\mathbf{P}, \mathbf{B}\right)$ on the n-th sub-band and the m-th user, as

$$\mathbf{H}\left(U_{m,n}\left(\mathbf{P}, \mathbf{B}\right)\right) = \begin{bmatrix} -\Lambda_1^{\mathrm{DL}} & \Lambda_1^{\mathrm{DL}} & 0 & 0 \\ \Lambda_1^{\mathrm{DL}} & -\Lambda_2^{\mathrm{DL}} & 0 & 0 \\ 0 & 0 & -\Lambda_1^{\mathrm{UL}} & \Lambda_1^{\mathrm{UL}} \\ 0 & 0 & \Lambda_1^{\mathrm{UL}} & -\Lambda_2^{\mathrm{UL}} \end{bmatrix}, \tag{4.14}$$

where

$$\Lambda_1^x = u_0 \eta_0 \cdot \frac{g_{m,n}^2 b_{m,n}^x}{\left(b_{m,n}^x N_0 + g_{m,n} p_{m,n}^x\right)^2 \ln 2},$$

and

$$\Lambda_2^x = u_m \eta_m \cdot \frac{\left(g_{m,n} p_{m,n}^x\right)^2}{\left(b_{m,n}^x N_0 + g_{m,n} p_{m,n}^x\right)^2 \ln 2}.$$

The four eigenvalues of the Hessian matrix are $\phi_1 = \phi_2 = 0$, $\phi_3 = -\left(\Lambda_1^{\mathrm{DL}} + \Lambda_2^{\mathrm{DL}}\right) \leq 0$, and $\phi_4 = -\left(\Lambda_1^{\mathrm{UL}} + \Lambda_2^{\mathrm{UL}}\right) \leq 0$. Since all its eigenvalues are nonpositive, the Hessian matrix is negative semi-definite. Therefore, we can conclude that $U_{m,n}\left(\mathbf{P}, \mathbf{B}\right)$ is jointly

https://doi.org/10.1017/9781108277389.005 Published online by Cambridge University Press

concave in $(\mathbf{P}, \mathbf{B})$, and $U(\mathbf{P}, \mathbf{B})$ is also jointly concave in $(\mathbf{P}, \mathbf{B})$ since linear operation preserves concavity.

In the expressions just discussed, we have proved that the objective function is a concave one. It is also rather obvious that the constraints also comprise a convex set. Thus, the problem is a convex one and standard convex tools, such as Lagrangian duality method, can be applied to solve it. The detailed steps of the convex optimization approach can be found in classical textbooks [20] and are therefore omitted.

In summary, the initial optimization problem in (4.10a) can be solved by two steps: the first one finds the optimal bandwidth and power allocation in (4.11) for given $(\boldsymbol{\beta}, \boldsymbol{u})$, and the second one finds the optimal $(\boldsymbol{\beta}^*, \boldsymbol{u}^*)$ that satisfies (4.12) and (4.13).

For the second step, we can develop a modified Newton method to solve it. We first introduce the following theorem, which can be proved in a similar way as Theorem 3.1 in [21].

THEOREM 4.2 *Let* $\psi_m(\boldsymbol{\beta}, \boldsymbol{u}) = -\eta_m R_m + \beta_m P_m$, $\psi_{M+1+m}(\boldsymbol{\beta}, \boldsymbol{u}) = -1 + u_m P_m$, $m = 0, 1, \cdots, M$, *and* $\boldsymbol{\psi}(\boldsymbol{\beta}, \boldsymbol{u}) = [\psi_0(\boldsymbol{\beta}, \boldsymbol{u}), \psi_1(\boldsymbol{\beta}, \boldsymbol{u}), \cdots, \psi_{2M+1}(\boldsymbol{\beta}, \boldsymbol{u})]$. *Then, the optimal* $(\boldsymbol{\beta}^*, \boldsymbol{u}^*)$ *is achieved if and only if*

$$\boldsymbol{\psi}(\boldsymbol{\beta}, \boldsymbol{u}) = \mathbf{0}. \tag{4.15}$$

Moreover, the optimal $(\boldsymbol{\beta}^*, \boldsymbol{u}^*)$ *is unique for problem (4.11).*

Furthermore, the modified Newton (MN) method can be used to solve the equation in (4.15), as expressed in the follows

$$\boldsymbol{\beta}^{k+1} = \boldsymbol{\beta}^k + \lambda_k \mathbf{q}^k, \, \boldsymbol{u}^{k+1} = \boldsymbol{u}^k + \lambda_k \mathbf{q}^k, \tag{4.16}$$

$$\mathbf{q}^k = -\left[\boldsymbol{\psi}'\left(\boldsymbol{\beta}^k, \boldsymbol{u}^k\right)\right]^{-1} \boldsymbol{\psi}\left(\boldsymbol{\beta}^k, \boldsymbol{u}^k\right), \tag{4.17}$$

where λ_k is the greatest ξ^i that satisfies

$$\left\| \boldsymbol{\psi}\left(\boldsymbol{\beta}^k + \xi^i \mathbf{q}^k, \boldsymbol{u}^k + \xi^i \mathbf{q}^k\right) \right\| \leq \left(1 - \epsilon \xi^i\right) \left\| \boldsymbol{\psi}\left(\boldsymbol{\beta}^k, \boldsymbol{u}^k\right) \right\|, \tag{4.18}$$

and $i \in \{0, 1, 2, \cdots\}$, $\xi \in (0, 1)$, and $\epsilon \in (0, 1)$. Specifically, $\boldsymbol{\beta}^{k+1}$ and $\boldsymbol{u}^{k+1}$ can also be expressed component-wise as

$$\beta_m^{k+1} = (1 - \lambda_k) \beta_m^k + \lambda_k \frac{\eta_m R_m^k}{P_m^k}, \, \forall m, \tag{4.19}$$

$$u_m^{k+1} = (1 - \lambda_k) u_m^k + \lambda_k \frac{1}{P_m^k}, \, \forall m. \tag{4.20}$$

In summary, the algorithm includes two loops: the inner loop is the optimal bandwidth and power allocation and the outer loop is the sum-of-ratios optimization that finds the optimal $(\boldsymbol{\beta}, \boldsymbol{u})$. As mentioned in Chapter 2, the sum-of-ratios algorithm is a global-optimal solution. Moreover, the inner loop is a standard convex problem and also its global optimum solution can be achieved. Therefore, our proposed algorithm can achieve the global optimal solution to the original problem in (4.10). Regarding

https://doi.org/10.1017/9781108277389.005 Published online by Cambridge University Press

Table 4.1 The global optimal solution for joint downlink and uplink resource allocation.

Algorithm 7 The global optimal solution for joint downlink and uplink resource allocation.

1: Initialize the maximum tolerance $\mathbf{\Delta}$ and the maximum number of iterations $I_{\max}$.
2: Choose $\xi \in (0,1)$, $\epsilon \in (0,1)$, and $(\mathbf{P}^0, \mathbf{B}^0) \in \mathbf{dom}\ EE$. Let

$$\beta_0^0 = \eta_0 \frac{\sum_{n=1}^{N}\sum_{m=1}^{M} b_{m,n}^{\mathrm{DL0}} \log_2\left(1+\frac{g_{m,n}p_{m,n}^{\mathrm{DL0}}}{b_{m,n}^{\mathrm{DL0}}N_0}\right)}{\sum_{n=1}^{N}\sum_{m=1}^{M} w_n p_{m,n}^{\mathrm{DL0}} + P^{\mathrm{DL,I}} + \sum_{n=1}^{N} P_n^{\mathrm{DL,D}} \sum_{m=1}^{M}\left(b_{m,n}^{\mathrm{DL0}} + b_{m,n}^{\mathrm{UL0}}\right)},$$

$$\beta_m^0 = \eta_m \frac{\sum_{n=1}^{N} b_{m,n}^{\mathrm{UL0}} \log_2\left(1+\frac{g_{m,n}p_{m,n}^{\mathrm{UL0}}}{b_{m,n}^{\mathrm{UL0}}N_0}\right)}{\sum_{n=1}^{N} v_n p_{m,n}^{\mathrm{UL0}} + P^{\mathrm{UL,I}} + \sum_{n=1}^{N}\left(b_{m,n}^{\mathrm{DL0}} + b_{m,n}^{\mathrm{UL0}}\right) P_n^{\mathrm{UL,D}}}, \forall m,$$

$$u_0^0 = \left(\sum_{n=1}^{N}\sum_{m=1}^{M} w_n p_{m,n}^{\mathrm{DL0}} + P^{\mathrm{DL,I}} + \sum_{n=1}^{N} P_n^{\mathrm{DL,D}} \sum_{m=1}^{M}\left(b_{m,n}^{\mathrm{DL0}} + b_{m,n}^{\mathrm{UL0}}\right)\right)^{-1},$$

$$u_m^0 = \left(\sum_{n=1}^{N} v_n p_{m,n}^{\mathrm{UL0}} + P^{\mathrm{UL,I}} + \sum_{n=1}^{N}\left(b_{m,n}^{\mathrm{DL0}} + b_{m,n}^{\mathrm{UL0}}\right) P_n^{\mathrm{UL,D}}\right)^{-1}, \forall m.$$

3: Initialize the iteration index $k = 0$. Denote $\boldsymbol{\beta}^k = \left(\beta_0^k, \cdots, \beta_M^k\right)$, $\boldsymbol{u}^k = \left(u_0^k, \cdots, u_M^k\right)$.
4: Find the optimal $\left(\mathbf{P}^k, \mathbf{B}^k\right)$ for a given $\left(\boldsymbol{\beta}^k, \boldsymbol{u}^k\right)$ by convex optimization tool.
5: **if** $\boldsymbol{\psi}\left(\boldsymbol{\beta}^k, \boldsymbol{u}^k\right) \preceq \mathbf{\Delta}$ **then**
6: $\left(\boldsymbol{P}^k, \boldsymbol{B}^k\right)$ is the optimal solution and stop the algorithm.
7: **else**
8: Denote i_k as the smallest i satisfying (4.18).
9: Let $\lambda_k = \xi^{i_k}$, update $\boldsymbol{\beta}^{k+1}$, $\boldsymbol{u}^{k+1}$ and $\mathbf{q}^k$ by (4.16), (4.17).
10: $k = k + 1$.
11: **if** $k < I_{\max}$ **then**
12: go to step 4.
13: **else**
14: go to step 16.
15: **end if**
16: **end if**

the computational complexity, the sum-of-ratios optimization algorithm converges in superlinear/quadratic rate and the subgradient method of convex optimization converges in linear rate [22]. Therefore, the computational complexity of the proposed algorithm is low and acceptable for practical implementation. The detailed procedures of the proposed algorithm are illustrated in Table 4.1.

https://doi.org/10.1017/9781108277389.005 Published online by Cambridge University Press

Table 4.2 System Parameters

Parameters	Settings
Noise	-174 dBm/Hz
User noise figure	9 dB
Base station noise figure	5 dB
Base station antenna gain	15 dBi
User antenna gain	0 dBi
Wavelength of sub-band 1, μ_1	0.375 m
Path loss of sub-band 1, α_1	3
Bandwidth of sub-band 1, W_1	4 MHz
Wavelength of sub-band 2, μ_2	0.12 m
Path loss of sub-band 2, α_2	4
Bandwidth of sub-band 2, W_2	8 MHz
$P^{\mathrm{DL,I}}$, $P^{\mathrm{UL,I}}$	46 dBm, 24.8 dBm
$P_1^{\mathrm{DL,D}}$, $P_1^{\mathrm{UL,D}}$	-23 dBm/Hz, -40 dBm/Hz
$P_2^{\mathrm{DL,D}}$, $P_2^{\mathrm{UL,D}}$	-26 dBm/Hz, -43 dBm/Hz
$P^{\mathrm{DL,max}}$, $P_m^{\mathrm{UL,max}}, \forall m$	46 dBm, 24 dBm
$\mathbf{\Delta}$, $\Delta^{'}$	$\left[10^{-4}, \cdots, 10^{-4}\right]$, 10^{-4}
$I_{\max}$, $I_{\max}^{'}$	5, 100
$R_m^{\mathrm{DL,min}}$, $R_m^{\mathrm{UL,min}}, \forall m$	10 Mbit/s
$w_n, v_n, n = 1,2$	1, 1
(ξ, ϵ)	(0.5, 0.5)

4.2.3 Numerical Results

In what follows, we shall provide numerical results to verify the proposed joint downlink and uplink energy-efficient resource allocation algorithm. In the simulation, we consider a single-cell network with a radius of 250 m. There are two sub-bands, sub-band 1 and sub-band 2, with different central frequencies of 800 MHz and 2.5 GHz, respectively. Four users are located in the network with distances of 50 m, 100 m, 150 m, and 200 m from the BS. The channel between the BS and users follows i.i.d Rayleigh model. Other major simulation parameters are given in Table 4.2 unless otherwise stated.

We first test the convergence speed of the proposed algorithm, as presented in Fig. 4.3. In this test, we set the same weight for all users, i.e., $\eta_m = \eta$, $m = 1,2,3,4$. We can observe from the figure that the sum-of-ratios optimization converges only after about 4–5 iterations, demonstrating a fast convergence speed of our proposal.

Figure 4.4 shows the bandwidth allocation on each sub-band with different weights of uplink EEs. In this test, we set the same weight to each uplink EE, i.e., $\eta_m = \eta, m = 1,2,3,4$. We also assume that sub-band 1 is more energy-efficient than sub-band 2 since sub-band 1 has a lower center frequency. From Fig. 4.4c, more bandwidth will be allocated to the uplink if more importance is put up to users than the BS. We can also observe that more bandwidth on sub-band 1 will be allocated to users with the increase of the weight value, η, to achieve higher uplink EE. Meanwhile, to

https://doi.org/10.1017/9781108277389.005 Published online by Cambridge University Press

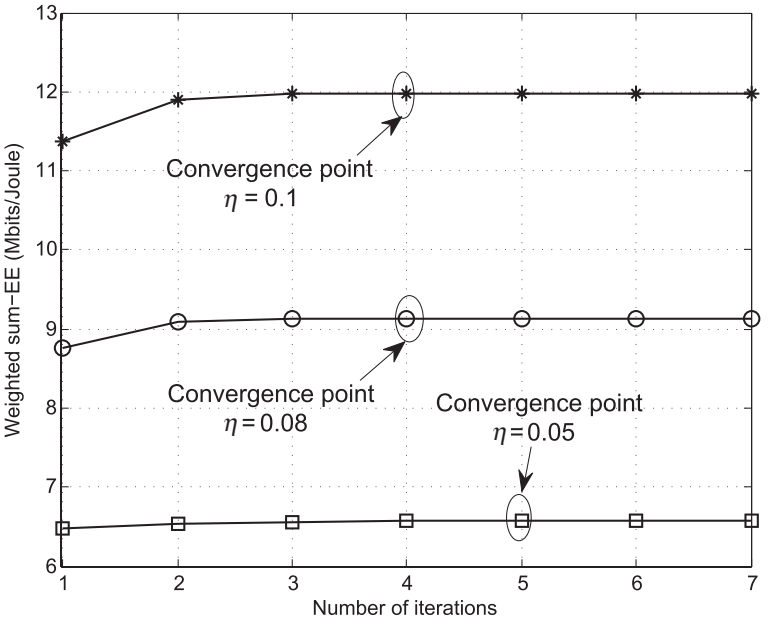

Figure 4.3 The convergence of the sum-of-ratios algorithm. © 2015 IEEE. Reprinted, with permission, from Yu, G., 2015, 'Joint Downlink and Uplink Resource Allocation for Energy-Efficient Carrier Aggregation', IEEE Transactions on Wireless Communications, Vol. 14, No. 6, pp. 3207–3218.

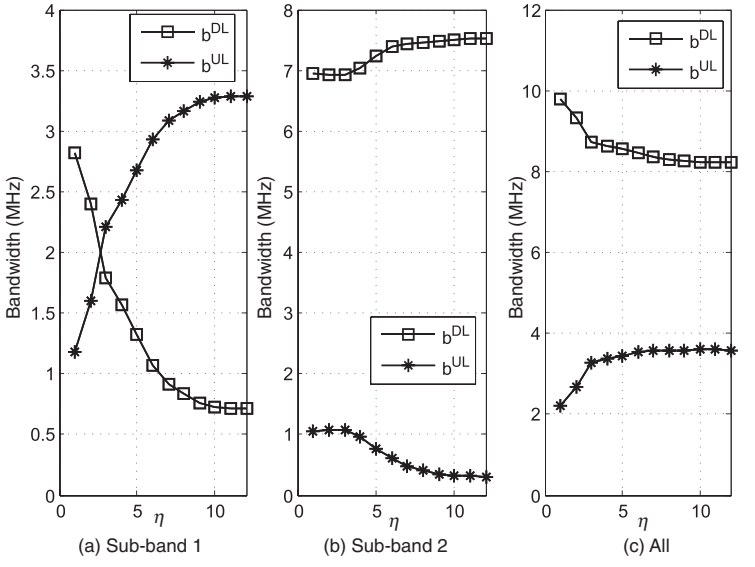

Figure 4.4 The bandwidth allocation for different weights of uplink EE. © 2015 IEEE. Reprinted, with permission, from Yu, G., 2015, 'Joint Downlink and Uplink Resource Allocation for Energy-Efficient Carrier Aggregation', *IEEE Transactions on Wireless Communications*, Vol. 14, No. 6, pp. 3207–3218.

https://doi.org/10.1017/9781108277389.005 Published online by Cambridge University Press

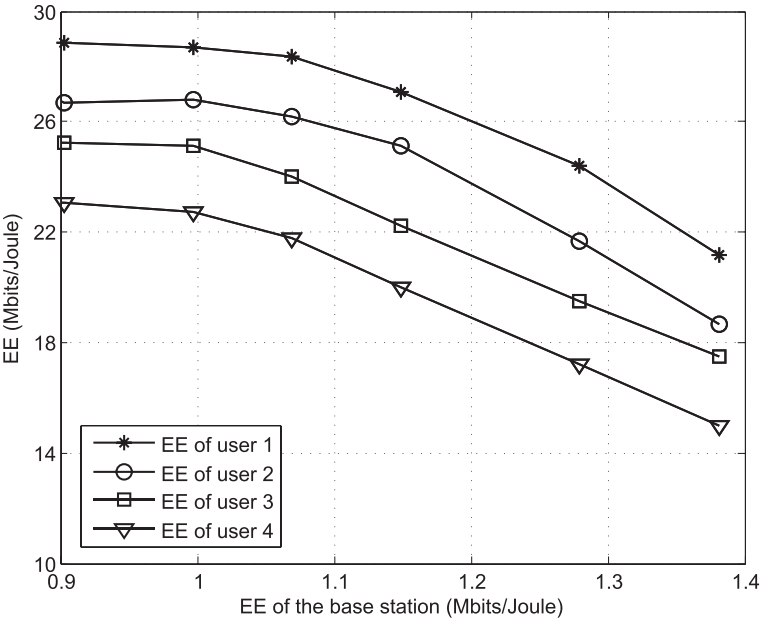

Figure 4.5 EE tradeoff between downlink and uplink. © 2015 IEEE. Reprinted, with permission, from Yu, G., 2015, 'Joint Downlink and Uplink Resource Allocation for Energy-Efficient Carrier Aggregation', *IEEE Transactions on Wireless Communications*, Vol. 14, No. 6, pp. 3207–3218.

guarantee the minimum data rate requirement, the downlink bandwidth on sub-band 2 will increase. Due to the same reason, the downlink bandwidth allocation will eventually remain at its minimum value as η goes large.

In Fig. 4.5, we assume that each user has the same weight, i.e., $\eta_m = \eta, m = 1,2,3,4$, and adjust η from 0.005 to 0.03. From the figure, a clear EE tradeoff between downlink and uplink can be observed. To further show the EE tradeoff among users, we fix $\eta_m = 0.05, m = 2,3,4$ while changing η_1 from 0.005 to 0.05, and the results are depicted in Fig. 4.6. From the figure, the EEs of other users, i.e., $\chi_m, m = 2,3,4$, decreases with the EE of user 1. Therefore, we can conclude that the proposed algorithm can achieve a flexible EE tradeoff between downlink and uplink as well as among different users.

4.3 Energy-Efficient Resource Allocation in Homogeneous Networks

In Chapter 2, we introduced several works on the energy-efficient design in single-cell networks, such as fundamental EE–SE tradeoff, EE design in OFDMA systems, and EE design in non-orthogonal systems. In this chapter, we will discuss the energy-efficient design in multicell systems where intercell interference poses a major challenge for EE design. We will first investigate multicell homogeneous networks with the same kind of LTE BSs. For such a scenario, there have been several algorithms to improve the overall system EE, which is defined as the ratio between the overall transmit data rate and the

https://doi.org/10.1017/9781108277389.005 Published online by Cambridge University Press

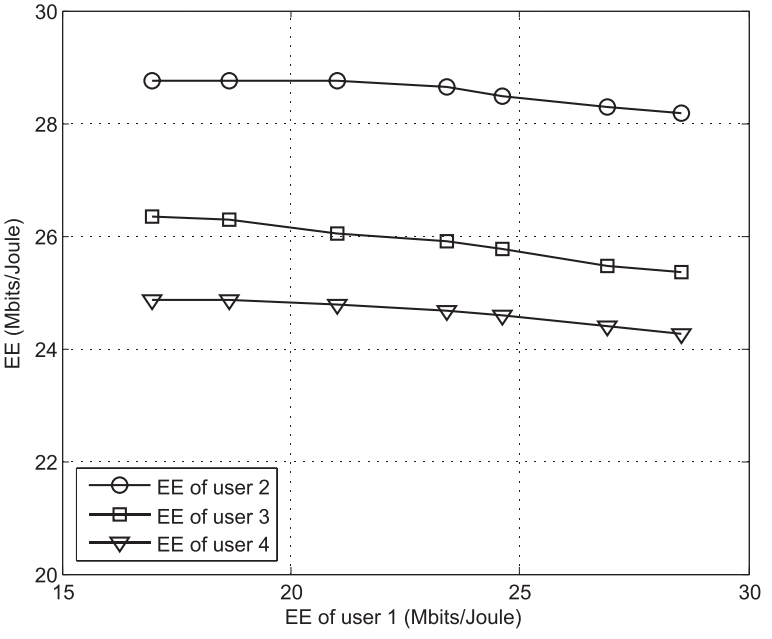

Figure 4.6 EE tradeoff among users. © 2015 IEEE. Reprinted, with permission, from Yu, G., 2015, 'Joint Downlink and Uplink Resource Allocation for Energy-Efficient Carrier Aggregation', *IEEE Transactions on Wireless Communications*, Vol. 14, No. 6, pp. 3207–3218.

overall energy consumption. In this section, we will utilize a more general EE objective, that is, to maximize the individual EE of each BS.

The motivation of this work is to maximize the individual EE of each BS, which has a more practical meaning than the overall EE maximization, as explained in the following. Currently, there exist some BSs powered by renewable external energy (e.g., solar and wind) in addition to those traditional BSs powered by the electricity grid. In such a situation, the EEs of different BSs may have different levels of importance. For example, to prolong the battery lifetime, BSs powered by external energy source should be more energy-efficient than those powered by the electricity grid. Therefore, it is more meaningful to consider the individual EE of each BS rather than the overall system EE. Nevertheless, the overall system EE maximization could be regarded as a special case of individual EE maximization.

In a multicell homogeneous network, the multi-stream aggregation (MSA) technique can be applied to improve the user data rate by aggregating data from different channels belonging to different BSs [23, 24]. This technique can greatly help improve the user experience of cell-edge users that can easily gather data from several nearby BSs. However, there are also many challenges related with the MSA technique. Among others, how to associate users with proper BSs, and how to allocate channel and power resource on each channel, are two critical challenges worth investigating. Several existing works have explored the user association and resource allocation algorithm in MSA systems

https://doi.org/10.1017/9781108277389.005 Published online by Cambridge University Press

from the perspective of system throughput maximization [25, 26]. However, there is no work considering the EE issue in such systems.

In the following subsection, we will first describe the system model and formulate the problem before introducing an effective algorithm to solve the problem. After that, we will provide numerical results to test our algorithm.

4.3.1 System Model and Problem Formulation

As depicted in Fig. 4.7, a multicell homogeneous system with K BSs and M users is investigated. The whole system has N orthogonal channels, and each has a bandwidth of W Hz. It is assumed that each user can receive data from several different BSs by the MSA technique.

Assuming user m is associated with the k-th BS on the n-th channel, we can express its received signal-to-interference-plus-noise ratio (SINR) as

$$\gamma_{mk}^{n} = \frac{p_{mk}^{n} h_{mk}^{n}}{WN_0 + \sum_{i=1, i\neq m}^{M} \sum_{j=1, j\neq k}^{K} p_{ij}^{n} h_{mj}^{n}}, \tag{4.21}$$

where h_{mk}^{n} denotes the channel power gain of the m-th user on the n-th channel at the k-th BS, p_{mk}^{n} is the transmit power on that channel, and N_0 is the power density of Gaussian noise. Based on this, the data rate of user m, that is associated with the k-th

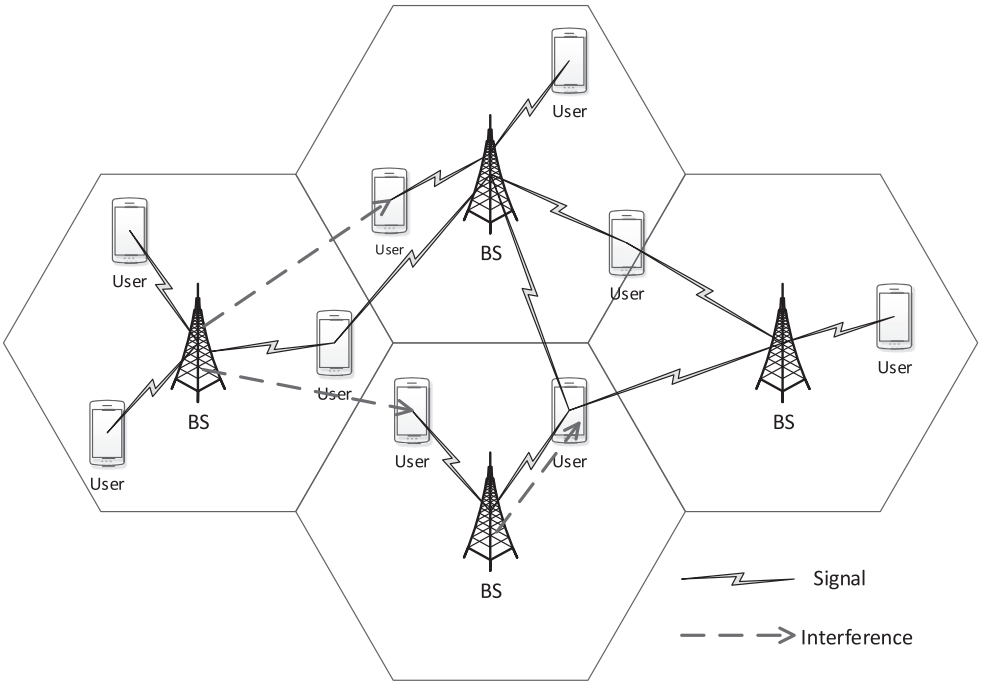

Figure 4.7 The network model for a homogenous cellular system with MSA.

https://doi.org/10.1017/9781108277389.005 Published online by Cambridge University Press

BS on the n-th channel, can be written as

$$R_{mk}^{n} = W \log \left(1 + \frac{p_{mk}^{n} h_{mk}^{n}}{WN_0 + \sum_{i=1, i\neq m}^{M} \sum_{j=1, j\neq k}^{K} p_{ij}^{n} h_{mj}^{n}} \right). \tag{4.22}$$

To calculate the EE of each BS, we should first figure out the overall data rate transmitted by the k-th BS as

$$R_k = \sum_{m=1}^{M} \sum_{n=1}^{N} \rho_{mk}^{n} R_{mk}^{n} . \tag{4.23}$$

In the above equation, ρ_{mk}^{n} denotes the binary user association and channel allocation indicator. That is, $\rho_{mk}^{n} = 1$ if user m is associated with the k-th BS, and the n-th channel is allocated to that user. Otherwise, $\rho_{mk}^{n} = 0$.

Similarly, the total transmit power of the k-th BS can be expressed as

$$P_k = \sum_{m=1}^{M} \sum_{n=1}^{N} \rho_{mk}^{n} p_{mk}^{n} . \tag{4.24}$$

Then, based on the definition of EE, we can express the EE of the k-th BS as

$$\varepsilon_k = \frac{R_k}{\omega_k \cdot P_k + P_k^{\mathrm{c}}}, \tag{4.25}$$

where ω_k and P_k^{c} denote the inverse of the power amplifier efficiency and the fixed circuit power consumption of the k-th BS, respectively.

As we have mentioned, we want to maximize the EE among different BSs with the constraints of user data rate requirement and the backhaul limit of each BS. Therefore, to indicate the levels of importance, we shall assign different weights to the EEs of different BSs. Let us denote η_k $(0 \leq \eta_k \leq 1)$ as the weight factor for the k-th BS, which is a fixed value determined by the network management utility. Let $\boldsymbol{\Omega}$ and $\boldsymbol{P}$ denote the resource and power allocation matrices with a dimensional of $M \times N \times K$, respectively. Then, we can mathematically formulate the optimization problem as

$$\max_{\{\boldsymbol{\Omega}, \mathbf{P}\}} \sum_{k=1}^{K} \eta_k \varepsilon_k, \tag{4.26}$$

subject to

$$\rho_{mk}^{n} \in \{0, 1\} \text{ and } \sum_{m=1}^{M} \rho_{mk}^{n} \leq 1, \forall k, n, \tag{4.26a}$$

$$\sum_{n=1}^{N} \sum_{k=1}^{K} \rho_{mk}^{n} R_{mk}^{n} \geq R_m^{\min}, \forall m, \tag{4.26b}$$

https://doi.org/10.1017/9781108277389.005 Published online by Cambridge University Press

$$\sum_{m=1}^{M}\sum_{n=1}^{N}\rho_{mk}^{n}p_{mk}^{n} \le P_{k}^{\max}, \forall k, \tag{4.26c}$$

$$\sum_{m=1}^{M}\sum_{n=1}^{N}\rho_{mk}^{n}R_{mk}^{n} \le R_{k}^{\max}, \forall k, \tag{4.26d}$$

$$p_{mk}^{n} \ge 0, \forall m, n, k. \tag{4.26e}$$

The above constraints include the orthogonality of channel allocation in each BS (4.26a), the minimum data rate requirement of each user (4.26b), the maximum transmit power limit (4.26c), and the backhaul capacity constraints of each BS (4.26d).

4.3.2 Problem Analysis and the Sub-Optimal Algorithm

We can observe that the problem in (4.26) is a sum-of-ratios optimization, since its objective function is the summation of several fractional functions, which is very complicated. Furthermore, this problem is also a combinatorial one due to the binary channel allocation matrix, $\mathbf{\Omega}$. Therefore, the problem is NP-hard and there exists no direct solution to solve it. To tackle it, we shall again leverage the sum-of-ratios optimization theory to convert it into a more tractable one, as presented in the following expressions.

First, the rate expression in (4.23) can be rewritten as

$$\begin{aligned} R_k &= \sum_{m=1}^{M}\sum_{n=1}^{N}\rho_{mk}^{n}W\log\left(1+\frac{p_{mk}^{n}h_{mk}^{n}}{WN_0+\sum\limits_{i=1,i\neq m}^{M}\sum\limits_{j=1,j\neq k}^{K}p_{ij}^{n}h_{mj}^{n}}\right) \\ &= \sum_{m=1}^{M}\sum_{n=1}^{N}W\log\left(1+\frac{\rho_{mk}^{n}p_{mk}^{n}h_{mk}^{n}}{WN_0+\sum\limits_{i=1,i\neq m}^{M}\sum\limits_{j=1,j\neq k}^{K}\rho_{mk}^{n}p_{ij}^{n}h_{mj}^{n}}\right), \forall k. \end{aligned} \tag{4.27}$$

Then, we can simply prove that $p_{mk}^{n}=0$ if $\rho_{mk}^{n}=0$. This is very clear that no power will be allocated if channel n of BS k is not allocated to user m. Based on this, the constraint in (4.23) is equivalent to

$$R_k = \sum_{m=1}^{M}\sum_{n=1}^{N}W\log\left(1+\frac{\rho_{mk}^{n}p_{mk}^{n}h_{mk}^{n}}{WN_0+\sum\limits_{i=1,i\neq m}^{M}\sum\limits_{j=1,j\neq k}^{K}\rho_{ij}^{n}p_{ij}^{n}h_{mj}^{n}}\right), \forall k. \tag{4.28}$$

https://doi.org/10.1017/9781108277389.005 Published online by Cambridge University Press

To deal with the combinatorial variable of ρ_{mk}^n, we can relax it into a continuous one, denoted as $\tilde{\rho}_{mk}^n$. Then, the initial problem in (4.26) can be converted into

$$\max_{\tilde{\mathbf{P}}} \sum_{k=1}^{K} \eta_k \tilde{\varepsilon}_k, \tag{4.29}$$

subject to

$$\sum_{n=1}^{N}\sum_{k=1}^{K} \tilde{R}_{mk}^n \geq R_m^{\min}, \forall m, \tag{4.29a}$$

$$\sum_{m=1}^{M}\sum_{n=1}^{N} \tilde{p}_{mk}^n \leq P_k^{\max}, \forall k, \tag{4.29b}$$

$$\sum_{m=1}^{M}\sum_{n=1}^{N} \tilde{R}_{mk}^n \leq R_k^{\max}, \forall k, \tag{4.29c}$$

$$\tilde{p}_{mk}^n \geq 0, \forall m, n, k, \tag{4.29d}$$

where

$$\tilde{p}_{mk}^n = \tilde{\rho}_{mk}^n p_{mk}^n,$$

$$\tilde{R}_{mk}^n = W \log\left(1 + \frac{\tilde{p}_{mk}^n h_{mk}^n}{WN_0 + \sum_{i=1, i\neq m}^{M} \sum_{j=1, j\neq k}^{K} \sum_{j=1, j\neq k} \tilde{p}_{ij}^n h_{mj}^n}\right),$$

$$\tilde{R}_k = \sum_{m=1}^{M}\sum_{n=1}^{N} \tilde{R}_{mk}^n,$$

$$\tilde{P}_k = \sum_{m=1}^{M}\sum_{n=1}^{N} \tilde{p}_{mk}^n,$$

and

$$\tilde{\varepsilon}_k = \frac{\tilde{R}_k}{\omega_k \cdot \tilde{P}_k + P_k^{\mathrm{c}}}.$$

Since the constraint in (4.26a) has been relaxed, the optimal solution to (4.29) is naturally larger than the optimal solution to the initial problem in (4.26). However, the modified problem is unfortunately non-concave, since the objective function is fractional, which is not concave. We shall utilize the sum-of-ratios optimization tool to transform the problem into a more tractable and equivalent one, as stated in the following theorem. The proof of this theorem can be found in the Appendix of Chapter 2.

https://doi.org/10.1017/9781108277389.005 Published online by Cambridge University Press

THEOREM 4.3 *If* $\tilde{\mathbf{P}}^*$ *is the optimal solution to (4.29), then there exist* $\boldsymbol{u}^* = \left(u_1^*, u_2^*, \cdots, u_K^*\right)$ *and* $\boldsymbol{\tau}^* = \left(\tau_1^*, \tau_2^*, \cdots, \tau_K^*\right)$ *such that* $\tilde{\mathbf{P}}^*$ *is a solution to the following problem under the constraints from (4.29a) to (4.29d) for* $\boldsymbol{u} = \boldsymbol{u}^*$ *and* $\boldsymbol{\tau} = \boldsymbol{\tau}^*$

$$\max_{\tilde{\mathbf{P}}} \sum_{k=1}^{K} u_k \left(\eta_k \tilde{R}_k - \tau_k(\omega_k \tilde{P}_k + P_k^{\mathrm{c}})\right). \tag{4.30}$$

Moreover, $\tilde{\mathbf{P}}^*$ *also satisfies the following system of equations for* $\boldsymbol{u} = \boldsymbol{u}^*$ *and* $\boldsymbol{\tau} = \boldsymbol{\tau}^*$*:*

$$u_k = \frac{1}{\omega_k \tilde{P}_k + P_k^{\mathrm{c}}}, k = 1, 2, \cdots, K. \tag{4.31}$$

$$\tau_k = \eta_k \tilde{\varepsilon}_k, k = 1, 2, \cdots, K. \tag{4.32}$$

According to the above theorem and the sum-of-ratios optimization theory (Section A2.1.2), we shall now solve the equivalent optimization problem in the sum-of-ratios subtractive form, i.e., $\max_{\tilde{\mathbf{P}}} \sum_{k=1}^{K} u_k \left(\eta_k \tilde{R}_k - \tau_k(\omega_k \tilde{P}_k + P_k^{\mathrm{c}})\right)$, for this case. We first analyze the property of the objective function in (4.30), which can be rewritten as

$$\begin{aligned} \tilde{R}_k = & \sum_{m=1}^{M}\sum_{n=1}^{N} W \log\left(WN_0 + \tilde{p}_{mk}^n h_{mk}^n + \sum_{i=1, i\neq m}^{M}\sum_{j=1, j\neq k}^{K} \tilde{p}_{ij}^n h_{mj}^n\right) \\ & - \sum_{m=1}^{M}\sum_{n=1}^{N} W \log\left(WN_0 + \sum_{i=1, i\neq m}^{M}\sum_{j=1, j\neq k}^{K} \tilde{p}_{ij}^n h_{mj}^n\right). \end{aligned} \tag{4.33}$$

Obviously, it is a summation of several difference-of-convex (d.c.) functions. Therefore, it is non-concave. To further solve the problem, we can utilize the successive convex approximation (SCA) approach to convert the objective function into the concave form. The main idea of the SCA method is to approximate the d.c. optimization problem into a series of convex optimization problems. The detailed approaches are described in the follows.

We can first express the lower bound of $\tilde{R}_k$ as

$$\tilde{R}_k = \sum_{m=1}^{M}\sum_{n=1}^{N} W \log\left(1 + \tilde{\gamma}_{mk}^n\right) \geq \sum_{m=1}^{M}\sum_{n=1}^{N} W\left(\alpha_{mk}^n \log(\tilde{\gamma}_{mk}^n) + \beta_{mk}^n\right), \tag{4.34}$$

which is tight when

$$\alpha_{mk}^n = \frac{\tilde{\gamma}_{mk}^n}{1 + \tilde{\gamma}_{mk}^n}, \tag{4.35}$$

$$\beta_{mk}^n = \log\left(1 + \tilde{\gamma}_{mk}^n\right) - \frac{\tilde{\gamma}_{mk}^n}{1 + \tilde{\gamma}_{mk}^n} \log(\tilde{\gamma}_{mk}^n). \tag{4.36}$$

Based on this, the objective function in (4.30) can be approximated into

$$\sum_{k=1}^{K} u_k \left(\eta_k \sum_{m=1}^{M}\sum_{n=1}^{N} W\left(\alpha_{mk}^n \log(\tilde{\gamma}_{mk}^n) + \beta_{mk}^n\right) - \tau_k(\omega_k \sum_{m=1}^{M}\sum_{n=1}^{N} \tilde{p}_{mk}^n + P_k^{\mathrm{c}})\right), \tag{4.37}$$

https://doi.org/10.1017/9781108277389.005 Published online by Cambridge University Press

for given approximation coefficients $\boldsymbol{\alpha} \triangleq \{\alpha_{mk}^n\}$ and $\boldsymbol{\beta} \triangleq \{\beta_{mk}^n\}$. We then define the auxiliary variable $\hat{p}_{mk}^n = \log(\tilde{p}_{mk}^n)$. Therefore, the initial problem in (4.29) can be eventually transformed into the following equivalent problems

$$\max_{\hat{\mathbf{P}}} \sum_{k=1}^{K} u_k \left[\eta_k \sum_{m=1}^{M} \sum_{n=1}^{N} W\left(\alpha_{mk}^n \log(\hat{\gamma}_{mk}^n) + \beta_{mk}^n\right) - \tau_k \left(\omega_k \sum_{m=1}^{M} \sum_{n=1}^{N} \exp\left(\hat{p}_{mk}^n\right) + P_k^{\mathrm{c}} \right) \right], \quad (4.38)$$

subject to

$$\sum_{n=1}^{N} \sum_{k=1}^{K} W\left(\alpha_{mk}^n \log(\hat{\gamma}_{mk}^n) + \beta_{mk}^n\right) \geq R_m^{\min}, \forall m, \quad (4.38a)$$

$$\sum_{m=1}^{M} \sum_{n=1}^{N} \exp\left(\hat{p}_{mk}^n\right) \leq P_k^{\max}, \forall k, \quad (4.38b)$$

$$\sum_{m=1}^{M} \sum_{n=1}^{N} W\left(\alpha_{mk}^n \log(\hat{\gamma}_{mk}^n) + \beta_{mk}^n\right) \leq R_k^{\max}, \forall k, \quad (4.38c)$$

where $\log(\hat{\gamma}_{mk}^n) = \hat{p}_{mk}^n + \log(h_{mk}^n) - \log\left(WN_0 + \sum_{i=1, i\neq m}^{M} \sum_{j=1, j\neq k}^{K} \exp\left(\hat{p}_{ij}^n\right) h_{mj}^n\right)$.

Now, the problem in (4.38) is eventually a convex problem due to the convexity of log-sum-exp functions. Thus, classical convex optimization approaches can be utilized to solve it. After the problem in (4.38) is solved, we still need the following operations. First, the optimal power should be transformed back according to $\tilde{p}_{mk}^n = \exp(\hat{p}_{mk}^n)$. Then, the bound in (4.37) should be iteratively updated until reaching a tighten one. Finally, the optimal $(\boldsymbol{u}^*, \boldsymbol{\tau}^*)$ should be updated according to the sum-of-ratios algorithm, i.e., iteratively updating $\boldsymbol{\alpha}$ and $\boldsymbol{\beta}$ until both (4.31) and (4.32) are satisfied.

In summary, the original problem can be solved by three nested iterative loops, as depicted in Fig. 4.8. The innermost loop is the optimal power allocation based on the standard Lagrangian solution. The intermediate loop is the SCA step that finds the appropriate $\left\{\alpha_{m,k}^n\right\}$ and $\left\{\beta_{m,k}^n\right\}$ to approximate $\tilde{R}_k$. The outermost loop is the sum-of-ratios algorithm, finding the optimal $(\boldsymbol{\tau}, \mathbf{u})$ that satisfies (4.31) and (4.32). This step can be realized by the Newton updating method as described earlier. Since all loops converge, the convergence of the whole algorithm can be guaranteed.

4.3.3 Numerical Results

In what follows, we shall provide numerical results to demonstrate the effectiveness of the proposed suboptimal algorithm. We adopt a simple scenario with two BSs and four users, where each BS covers a circle area with a radius of 500 m. There are four channels in each BS and users are randomly located in the network. An independent Rayleigh channel model is used to model the channel fading between the BSs and the users. The other major simulation parameters are summarized in Table 4.3.

We first test the convergence performance of the proposed algorithm. Figures 4.9(a) and 4.9(b) show the convergence rate of the sum-of-ratios algorithm (the outermost loop) and the SCA algorithm (the intermediate loop), respectively. From the figure, both

https://doi.org/10.1017/9781108277389.005 Published online by Cambridge University Press

Table 4.3 Simulation Parameters

Parameters	Settings
Cellular radius	500 m
Noise	−174 dBm/Hz
Path loss exp.	3.5
$P_k^{\mathrm{c}}, \forall k$	40 W
$R_k^{\max}, \forall k$	50 Mbit/s
$w_k, \forall k$	1
W	1 MHz
$P_k^{\max}$	2.6 W

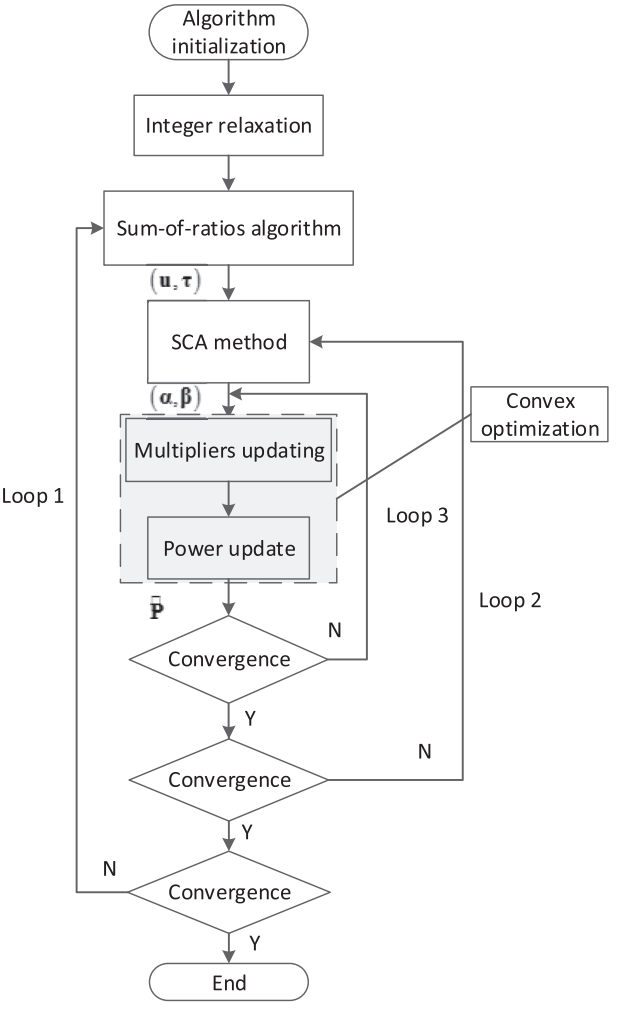

Figure 4.8 Block diagram of the suboptimal algorithm.

https://doi.org/10.1017/9781108277389.005 Published online by Cambridge University Press

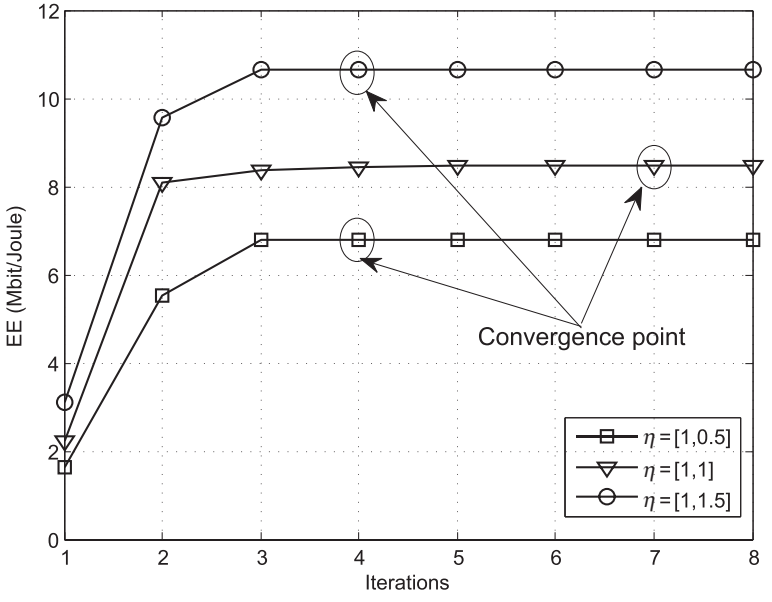

(a) The sum-of-ratios algorithm.

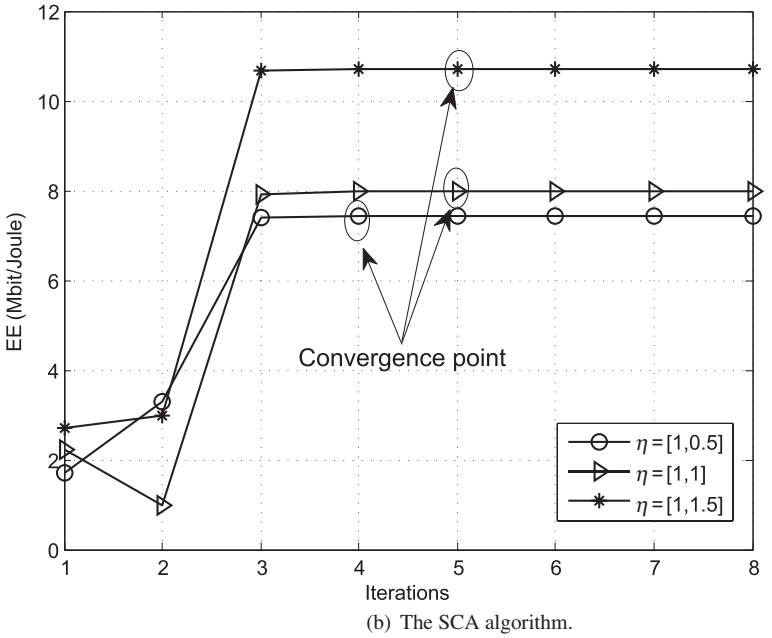

(b) The SCA algorithm.

Figure 4.9 The convergence performance of the sum-of-ratios and SCA algorithms. (a) The sum-of-ratios algorithm. (b) The SCA algorithm. © 2016 IEEE. Reprinted, with permission, from Chen, Q., 2016, 'Energy-Efficient User Association and Resource Allocation for Multistream Carrier Aggregation', *IEEE Transactions of Vehicular Technology*, vol. 65, no. 8, pp. 6366–6376.

https://doi.org/10.1017/9781108277389.005 Published online by Cambridge University Press

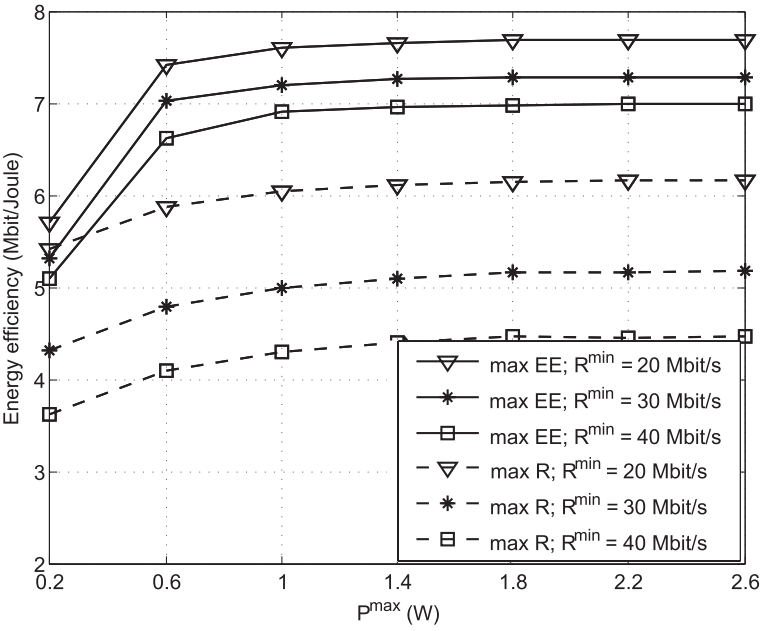

Figure 4.10 EE comparison between the EE-optimal algorithm and the rate-optimal algorithm. © 2016 IEEE. Reprinted, with permission, from Chen, Q., 2016, 'Energy-Efficient User Association and Resource Allocation for Multistream Carrier Aggregation', *IEEE Transactions of Vehicular Technology*, vol. 65, no. 8, pp. 6366–6376.

algorithms only require a few iterations to reach the optimal solutions, demonstrating the quick convergence of our proposed algorithms.

We then compare the proposed EE-optimal algorithm with the rate-optimal algorithm that aims to maximize the overall system throughput. Note that the rate-optimal algorithm can be designed by simply replacing the objective function with the overall system data rate. It can be also achieved by the SCA algorithm with the standard convex optimization in a similar way. Figures 4.10 and 4.11 illustrate the EE performance and data rate performance of our proposed algorithm, respectively, as compared with the rate-optimal algorithm. As depicted in the figures, although the rate-optimal algorithm can maximize the overall system throughput, the EE-optimal algorithm can achieve a better EE with a small loss of data rate. It shows that our proposal can indeed achieve a higher EE and higher system throughput simultaneously.

4.4 Energy-Efficient Resource Allocation in Heterogenous Networks

So far, we have discussed the energy-efficient resource allocation for the homogenous cellular system with multiple macro-cell BSs. With the dramatic increase of mobile data traffic, the cellular network structure is undergoing major changes. In addition to those macro-cell BSs, various kinds of low-power access points have been deployed to

https://doi.org/10.1017/9781108277389.005 Published online by Cambridge University Press

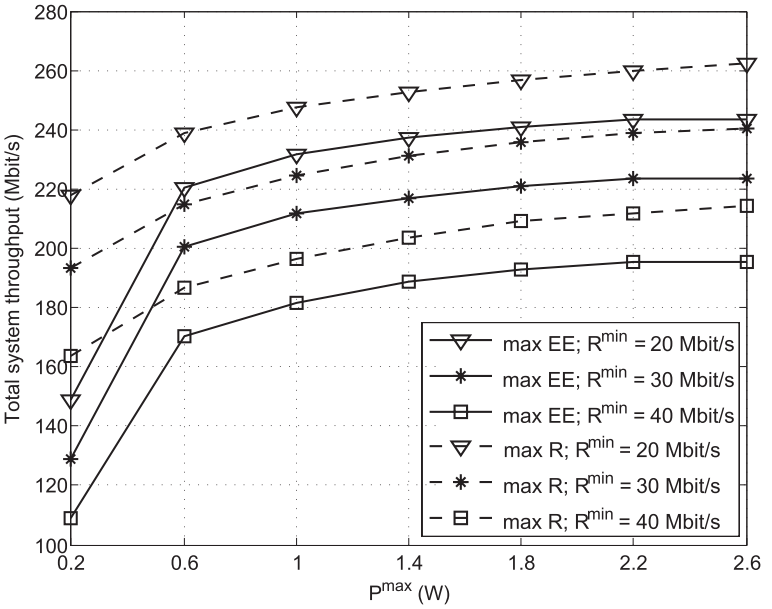

Figure 4.11 System throughput comparison between the EE-optimal algorithm and the rate-optimal algorithm. © 2016 IEEE. Reprinted, with permission, from Chen, Q., 2016, 'Energy-Efficient User Association and Resource Allocation for Multistream Carrier Aggregation', *IEEE Transactions of Vehicular Technology*, vol. 65, no. 8, pp. 6366–6376.

improve network capacity, which is referred to as heterogeneous wireless networks [27]. Besides the improvement on the area spectral efficiency because of dense frequency reuse, the EE can also be enhanced due to the low-power transmitter. There are two kinds of heterogeneous networks (HetNets), namely single-RAT HetNets and multi-RAT HetNets. The access points of the former one belong to the same RAT, e.g., LTE macro-cell, pico-cell, and femto-cell. On the other hand, the latter one consists of different access points with different radio access technologies, such as the coexistence of LTE BSs and WiFi access points. The major characteristic of the multi-RAT heterogenous network (HetNet) is that different access points are usually deployed by different operators and work on different frequency bands. This brings new communication freedom into multi-RAT mobile devices to dynamically and optimally select the most suitable network for better performances. Moreover, users can also utilize the multi-homing technology to further improve the throughput by aggregating data from different networks. Therefore, the multi-RAT HetNet has aroused considerable research interest in recent years.

Undoubtedly, the EE of both single-RAT and multi-RAT HetNets is also an important issue worth investigation [28]. Early studies show that, by offloading cellular traffic to the WiFi network, both system capacity and EE can be significantly improved [29–31]. The works in [32, 33] proposed partial spectrum reuse and adaptive BS sleeping control strategies to improve the EE of two-tier heterogeneous networks, respectively. In [34, 35], energy-efficient coordinated beamforming and precoding schemes have

https://doi.org/10.1017/9781108277389.005 Published online by Cambridge University Press

been proposed to maximize the system-level EE of MIMO heterogeneous networks. The large-scale user behavior and traffic dynamics can also be leveraged to design energy-efficient communication protocols [36, 37]. Moreover, energy-efficient optimal access point selection [38] and resource allocation algorithms [39] for multi-RAT heterogeneous networks have been investigated.

In this section, we will introduce energy-efficient joint bandwidth and power allocation for multi-RAT HetNets to maximize the EE of uplink users. In contrast to existing works that generally maximize the system-level EE, we aim at maximizing the EE of each individual user. This objective is much more general than the overall EE and has the merit of providing a better understanding of EE tradeoff. The problem of maximizing the overall EE is generally a fractional programming problem. However, maximizing all uplink EEs is much more different and new methods should be involved. Therefore, we introduce a multi-objective optimization tool to model the individual EE maximization problem. To deal with it, we first propose a novel concept of utopia EE for each user, defined as the maximum EE that a particular user can achieve. After that, we develop an effective multi-objective resource allocation algorithm based on the weighted Tchebycheff method.

In what follows, we will first introduce the multi-RAT HetNet and formulate the optimization problem. Then, we will describe the concept of Utopia EE and devise the novel algorithm to solve the problem. Finally, numerical results will be provided to demonstrate the performance of the proposed algorithm.

4.4.1 System Model and Problem Formulation

The system model of multi-RAT HetNets is depicted in Fig. 4.12. The system has M ($M \in \mathcal{M} = \{1, 2, \ldots, M\}$) different types of access points (APs), each equipped with

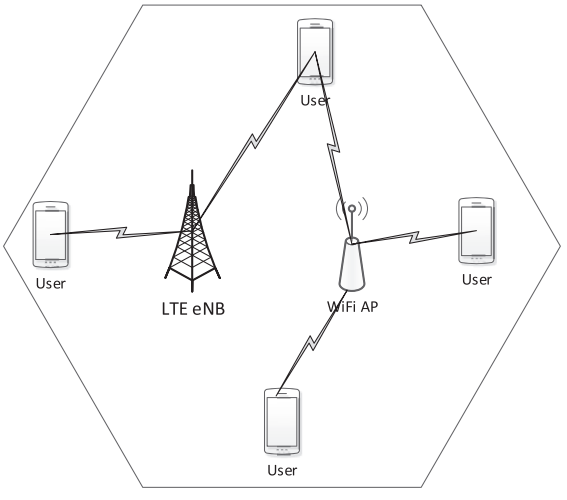

Figure 4.12 System model for multi-RAT heterogenous networks.

https://doi.org/10.1017/9781108277389.005 Published online by Cambridge University Press

different RAT. For example, there are three different access points, namely, LTE BS, LTE-A small-cell access point, and WiFi access point. Different APs work on different frequency bands and thus inter-RAT interference does not exist. There are N ($N \in \mathcal{N} = \{1, 2, \ldots, N\}$) users randomly distributed in the network. It is assumed that each user can utilize the multi-homing technology to opportunistically choose several APs. This can be implemented by splitting the data stream into multiple sub-streams, and each sub-stream is transmitted via one RAT. For simplicity, both APs and users are assumed to be equipped with one antenna, while our work can be easily extended to the multi-antenna scenario with few modification.

The overall available bandwidth of the m-th RAT is denoted as W_m, which can be allocated to all users associated with this RAT. Moreover, we have the channel power gain model between user n and RAT m as

$$g_{m,n} = h_{m,n} d_{m,n}^{-\alpha_m},$$

which is a function of the distance between user n and RAT m ($d_{m,n}$), the small-scale channel fading coefficient ($h_{m,n}$), and the path-loss exponent α_m. To perform the bandwidth and power allocation, it is assumed that all channel state information (CSI) is accurate and known at the centralized scheduler.

Let $b_{m,n}$ be the bandwidth allocated for user n in RAT m. Then, the achievable data rate for user n in RAT m can be modeled as

$$R_{m,n} = b_{m,n} \log_2(1 + SNR_{m,n}), \forall m, n, \tag{4.39}$$

where $SNR_{m,n}$ is the uplink SNR that can be expressed as a function of power allocation $p_{m,n}$ and channel power gain $g_{m,n}$, as

$$SNR_{m,n} = \frac{p_{m,n} g_{m,n}}{b_{m,n} N_0}, \forall m, n. \tag{4.40}$$

Then, the overall achievable data rate for user n can be written as

$$R_n = \sum_{m=1}^{M} b_{m,n} \log_2 \left(1 + \frac{p_{m,n} g_{m,n}}{b_{m,n} N_0}\right), \forall n. \tag{4.41}$$

Similar to the previous analysis, the power consumption for each user can be modelled as

$$P_n = \sum_{m=1}^{M} \omega_{m,n} p_{m,n} + P^{\mathrm{I}} + \sum_{m=1}^{M} b_{m,n} P_m^{\mathrm{D}}, \forall n. \tag{4.42}$$

Again, the power consumption model consists of three items: the transmit power with $\omega_{m,n}$ being the inverse of the power amplifier efficiency; the fixed power consumption; and the power consumption as a function of the occupied bandwidth, where P_m^{D} denotes the fixed power consumption if RAT m is used. We shall note that this model is more general than that in [39] in which the last item is not considered.

https://doi.org/10.1017/9781108277389.005 Published online by Cambridge University Press

According to (4.42), the EE of user n can be expressed as

$$\eta_n = \frac{R_n}{P_n}, \forall n. \tag{4.43}$$

As mentioned earlier, we aim at maximizing the EE for each individual user by joint bandwidth and power allocation. Therefore, the optimization problem can be formulated as

$$\max_{\mathbf{P},\mathbf{B}} \ \{\eta_1, \eta_2, \cdots, \eta_N\}, \tag{4.44}$$

subject to

$$\sum_{n=1}^{N} b_{m,n} \leq W_m, \forall m, \tag{4.44a}$$

$$\sum_{m=1}^{M} p_{m,n} \leq P_n^{\max}, \forall n, \tag{4.44b}$$

$$\sum_{m=1}^{M} R_{m,n} \geq R_n^{\min}, \forall n, \tag{4.44c}$$

$$b_{m,n} \geq 0, \ p_{m,n} \geq 0, \forall m, n. \tag{4.44d}$$

In the above problem, the optimization variables are $\mathbf{P} = \left\{p_{m,n}\right\}_{M\times N}$ and $\mathbf{B} = \left\{b_{m,n}\right\}_{M\times N}$, the constraint in (4.44a) limits the overall available bandwidth in each RAT, the constraint in (4.44b) is the maximum allowable transmit power of each user, and the constraint in (4.44c) guarantees the minimum uplink data rate requirement of users. Here, the problem is assumed to be always feasible. This can be achieved by proper admission control strategies.

Equation (4.44) and its four parts are a multi-objective optimization problem [40], which aims to maximize several different objective functions. Since EEs of all users cannot be maximized simultaneously, those objective functions are generally conflicting with each other. Therefore, the optimal solutions are in general Pareto-optimal, which indicates that one cannot improve the EE of one user without decreasing the EE of other users. Different from a single-objective optimization problem, there may exist many Pareto-optimal solutions to a multi-objective optimization problem in general. For our case, Pareto-optimal EE can be defined as follows.

Pareto optimal EE: *An EE vector $\eta^* = \{\eta_1^*, \eta_2^*, \cdots, \eta_N^*\}$ is Pareto-optimal if and only if there does not exist another EE vector η such that $\eta_n \geq \eta_n^*$ for all users, but $\eta_i > \eta_i^*$ for at least one user.*

4.4.2 The Multi-Objective Energy-Efficient Algorithm

Now we will try to develop a bandwidth and power allocation algorithm to achieve Pareto-optimal EE. Before solving it, we first introduce the concept of Utopia EE for each individual user, defined as.

https://doi.org/10.1017/9781108277389.005 Published online by Cambridge University Press

Utopia EE: *The Utopia EE for each user can be defined as the maximal EE it can achieve, i.e.,* $\eta_n^o = \max_{\eta \in \mathcal{F}} \{\eta_n\}$*, where* $\mathcal{F}$ *denotes the feasible set of bandwidth and power allocation strategies.*

Based on this definition, we can formulate the following optimization problem to find the Utopia EE for user n

$$\max_{\mathbf{P},\mathbf{B}} \ \eta_n, \tag{4.45}$$

subject to (4.44a)–(4.44d).

Clearly, this problem is a standard convex fractional programming, and therefore the classical Dinkelbach algorithm described in Chapter 2 can be utilized to solve it. The detailed procedures are omitted. After Utopia EE is solved for each user, we can convert the multiple-objective optimization problem into a single-objective one by utilizing the weighted Tchebycheff method as described in Chapter 2. The objective function of the single-objective optimization problem can be written as

$$\min_{\mathbf{P},\mathbf{B}} \max_{n} \ \left\{\phi_n(\eta_n^o - \eta_n)\right\}, \tag{4.46}$$

where $\boldsymbol{\phi} = \{\phi_1, \cdots, \phi_N\}$ is any weight vector with all positive elements. By changing the weight vector, one can achieve all Pareto-optimal solutions from the above formulation. The equivalence between (4.46) and (4.44) is given in the following theorem.

THEOREM 4.4 *Let an EE vector* η *be a Pareto optimal solution to problem (4.44). Then, there must exist a positive weight vector* $\boldsymbol{\phi} = \{\phi_1, \cdots, \phi_N\}$*, such that* η *is the solution to problem (4.46).*

The relationship between Pareto-optimal EE and Utopia EE for a two-user case is depicted in Fig. 4.13. The shadowing area in this figure illustrates the feasible EE region for the problem in (4.44), and the upper bound of the region is the Pareto-optimal EE set. Moreover, the points of η_1^o and η_2^o are the two Utopia EE for user 1 and user 2, respectively. The point (η_1^*, η_2^*) is the Pareto optimal EE corresponding to the same weight vector, i.e., $\phi_1 = \phi_2$. From the figure, point (η_1^*, η_2^*) can achieve the minimum of $\max\{\eta_1^o - \eta_1^*, \eta_2^o - \eta_2^*\}$, as demonstrated in Theorem 4.4. Other Pareto-optimal EE points can be also achieved by setting different ϕ_i, for $i = 1, 2$, in a similar way. Indeed, the weight value ϕ_n reflects the different levels of importance for each user, which can be predetermined by the network operator according to practical applications. For example, one can assign a larger weight to those users with lower battery power or higher priority. In this way, the EEs for these users will be much closer to their maximum/Utopia EEs, as can be derived in the above Theorem 4.4.

Now we will develop an iterative algorithm to solve the problem in (4.46). First, inserting (4.43) into (4.46), the objective function can be converted into

$$\min_{\mathbf{P},\mathbf{B}} \max_{n} \ \left\{\phi_n \left(\frac{\eta_n^o P_n - R_n}{P_n}\right)\right\}. \tag{4.47}$$

https://doi.org/10.1017/9781108277389.005 Published online by Cambridge University Press

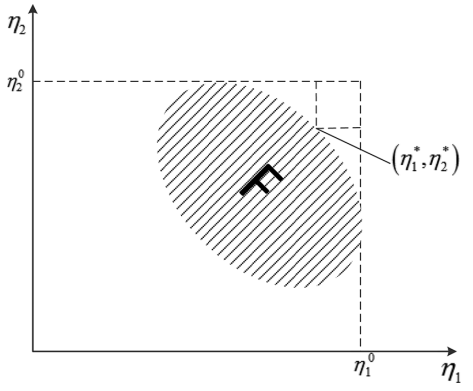

Figure 4.13 The illustration of Utopia EE and Pareto-optimal EE.

Now this problem becomes a generalized fractional programming (GFP), aiming at maximizing the minimum of several fractional functions [41, 42]. We can further prove that the objective function is quasiconvex and can be transformed into an equivalent but more tractable one, as shown in the following theorem.

THEOREM 4.5 *The objective function in (4.47) is quasiconvex and equivalent to*

$$\max_{\mathbf{y}\in\mathcal{Y}} \min_{\mathbf{P},\mathbf{B}} f(\mathbf{y},\mathbf{B},\mathbf{P}) = \frac{\sum_{n=1}^{N} y_n \phi_n(\eta_n^o P_n - R_n)}{\sum_{n=1}^{N} y_n P_n}, \tag{4.48}$$

where $\mathcal{Y} \triangleq \{(y_1, \cdots, y_N) | y_n \geq 0, \forall n, \sum_{n=1}^{N} y_n = 1\}$.

Proof First, we will show that $R_{m,n}$ is concave over $b_{m,n}$ and $p_{m,n}$. Define $x \triangleq b_{m,n}, y \triangleq \frac{p_{m,n} g_{m,n}}{N_0}$, and $f(x,y) = -x\log_2\left(1 + \frac{y}{x}\right)$.

The Hessian of $f(x,y)$ is

$$\mathbf{H} = \begin{bmatrix} \frac{y^2/x}{(x+y)^2} & -\frac{y}{(x+y)^2} \\ -\frac{y}{(x+y)^2} & \frac{x}{(x+y)^2} \end{bmatrix},$$

which is positive semi-defined, since its eigenvalues are

$$\lambda_1 = 0,$$
$$\lambda_2 = \frac{x^2 + y^2}{x^3 + 2x^2 y + x y^2} \geq 0\,.$$

Therefore, $R_{m,n} = -f(x,y)$ is concave and R_n is also concave since it is a linear combination of $R_{m,n}$.

To prove the quasiconvexity of (4.47), we write the sublevel set of $-\frac{R_n}{P_n}$ as

$$\tau_\alpha = \left\{ b_{m,n} \geqslant 0, p_{m,n} \geqslant 0, \forall m,n \,\middle|\, -\frac{R_n}{P_n} \leq \alpha \right\},$$

https://doi.org/10.1017/9781108277389.005 Published online by Cambridge University Press

which is equal to

$$\tau_\alpha = \left\{ b_{m,n} \geqslant 0, p_{m,n} \geqslant 0, \forall m, n \,|-\alpha P_n - R_n \leq 0 \right\} .$$

We see that τ_α is convex due to the convexity of $-\alpha P_n - R_n$, which leads to the quasiconvexity of $\eta_n^o - \frac{R_n}{P_n}$. According to [20], $\max_n \left\{ \phi_n \left(\frac{\eta_n^o P_n - R_n}{P_n} \right) \right\}$ is also quasiconvex.

Then, due to the fact that a quasiconvex function will attain its maximum in a vertex of a convex polyhedron [43], we have

$$\max_n \left\{ \phi_n \left(\frac{\eta_n^o P_n - R_n}{P_n} \right) \right\} = \max_{\mathbf{y} \in \mathcal{Y}} \frac{\sum_{n=1}^N y_n \phi_n (\eta_n^o P_n - R_n)}{\sum_{n=1}^N y_n P_n}.$$

We will now show that $f(\mathbf{y}, \mathbf{B}, \mathbf{P})$ is quasiconvex over $(\mathbf{B}, \mathbf{P})$ and quasilinear over $\mathbf{y}$.

For a given $\mathbf{y}$, the sublevel set of $f(\mathbf{y}, \mathbf{B}, \mathbf{P})$ can be denoted as

$$\tau_\alpha = \left\{ b_{m,n} \geqslant 0, p_{m,n} \geqslant 0, \forall m, n | f(\mathbf{y}, \mathbf{B}, \mathbf{P}) \leq \alpha \right\} .$$

Furthermore, we can rewrite $f(\mathbf{y}, \mathbf{B}, \mathbf{P}) \leq \alpha$ as

$$\sum_{n=1}^N y_n (\phi_n (\eta_n^o P_n - R_n) - \alpha P_n) \leq 0 .$$

Therefore, it can be easily observed that τ_α is convex since $\sum_{n=1}^N y_n (\phi_n (\eta_n^o P_n - R_n) - \alpha P_n)$ is convex over $(\mathbf{B}, \mathbf{P})$, which leads to the quasiconvexity of $f(\mathbf{y}, \mathbf{B}, \mathbf{P})$ over $(\mathbf{B}, \mathbf{P})$.

Again, for a given $(\mathbf{B}, \mathbf{P})$, the sublevel set of $f(\mathbf{y}, \mathbf{B}, \mathbf{P})$ is

$$S_\alpha = \left\{ y_n \geqslant 0, \forall n | f_y(\mathbf{y}) \leq \alpha \right\}, \tag{4.49}$$

which equals to

$$S_\alpha = \left\{ y_n \geqslant 0, \forall n | \sum_{n=1}^N y_n (\phi_n (\eta_n^o P_n - R_n) - \alpha P_n) \leq 0 \right\}.$$

Due to that $\sum_{n=1}^N y_n (\phi_n (\eta_n^o P_n - R_n) - \alpha P_n)$ is an affine function of $\mathbf{y}$, which is both convex and concave, $f(\mathbf{y}, \mathbf{B}, \mathbf{P})$ is quasilinear over $\mathbf{y}$.

Then, according to Sion's mini-max theorem [44], (4.47) can be finally converted into

$$\max_{\mathbf{y} \in \mathcal{Y}} \min_{\mathbf{P}, \mathbf{B}} f(\mathbf{y}, \mathbf{B}, \mathbf{P}).$$

This ends the proof. □

According to Theorem 4.6, we can obtain the optimal solution to the problem in (4.46) by iteratively solving the following two subproblems: a) finding the optimal

https://doi.org/10.1017/9781108277389.005 Published online by Cambridge University Press

$\{\mathbf{B}^*, \mathbf{P}^*\}$ for a given $\mathbf{y}$; b) finding the optimal $\mathbf{y}$. Mathematically, they can be respectively formulated as

$$\eta(\mathbf{y}) = \min_{\mathbf{P},\mathbf{B}} \ f(\mathbf{y}, \mathbf{B}, \mathbf{P}),$$

and

$$\eta^* = \max_{\mathbf{y}\in\mathcal{Y}} \ \eta(\mathbf{y}).$$

We can use the Dinkelbach algorithm [45] to solve the above problem where the optimal η^* should satisfy $U^* = 0$. However, it is very hard to directly find the optimal η^* to satisfy this condition. In what follows, we shall present an effective algorithm to solve the above two subproblems, as presented in the following theorem.

THEOREM 4.6 *Define*

$$U(\mathbf{y}, \alpha) = \sum_{n=1}^{N} y_n(\phi_n(\eta_n^o P_n - R_n) - \alpha P_n),$$

and let $\mathbf{y}^{(k)}, k = 0, 1, \cdots,$ *be a sequence updated by the following equation for any initial* $\mathbf{y}^{(0)}$*:*

$$\mathbf{y}^{(k+1)} = \arg\max_{\mathbf{y}\in\mathcal{Y}} \min_{\mathbf{P},\mathbf{B}} U(\mathbf{y}, \eta(\mathbf{y}^{(k)})).$$

Then we have

(a) For the first subproblem, $\eta(\mathbf{y})$ *is achieved when*

$$\min_{\mathbf{P},\mathbf{B}} U(\mathbf{y}, \eta(\mathbf{y})) = 0.$$

(b) For the second subproblem, we have $\eta(\mathbf{y}^{(k+1)}) \geq \eta(\mathbf{y}^{(k)})$ *and the optimal solution* $\eta^* = \eta(\mathbf{y}^{(k)})$ *is achieved when* $\eta(\mathbf{y}^{(k+1)}) = \eta(\mathbf{y}^{(k)})$*. In this case,*

$$U^* \triangleq \max_{\mathbf{y}\in\mathcal{Y}} \min_{\mathbf{P},\mathbf{B}} U(\mathbf{y}, \eta^*) = 0.$$

Proof The first subproblem is a standard concave fractional programming problem, thus (a) can be easily proved, based on the parametric algorithm in [45] by introducing the parameter α and the function $U(\mathbf{y}, \alpha)$.

For the second part, since

$$\eta(\mathbf{y}^{(k+1)}) = \min_{\mathbf{P},\mathbf{B}} f(\mathbf{y}^{(k+1)}, \mathbf{B}, \mathbf{P}),$$

we have

$$\min_{\mathbf{P},\mathbf{B}} U(\mathbf{y}^{(k+1)}, \eta(\mathbf{y}^{(k+1)})) = 0. \tag{4.50}$$

On the other hand, according to the definition of $\mathbf{y}^{(\mathbf{k+1})}$,

$$\min_{\mathbf{P},\mathbf{B}} U(\mathbf{y}^{(k+1)}, \eta(\mathbf{y}^{(k)})) \geq \min_{\mathbf{P},\mathbf{B}} U(\mathbf{y}^{(k)}, \eta(\mathbf{y}^{(k)})) = 0. \tag{4.51}$$

https://doi.org/10.1017/9781108277389.005 Published online by Cambridge University Press

Table 4.4 The algorithm to achieve Pareto-optimal EE

Algorithm 8 The algorithm to achieve the Pareto optimal EE

1: Initialize $\mathbf{y}^{(0)} \in \mathcal{Y}$, η, $k = 0$, ϵ_1, and ϵ_2.
2: Find $\{\mathbf{P}^*, \mathbf{B}^*\} = \arg\min_{\mathbf{P},\mathbf{B}} U(\mathbf{y}^{(\mathbf{k})}, \eta)$.
3: **If** $\left| \sum_{n=1}^{N} y_n^{(k)} (\phi_n(\eta_n^o P_n^* - R_n^*) - \eta P_n^*) \right| < \epsilon_1$, **then**
4: Set $\eta(\mathbf{y}^{(\mathbf{k})}) = \eta$.
5: **goto** step (10).
6: **Else**
7: Update $\eta = \frac{\sum_{n=1}^{N} y_n^{(k)} \phi_n(\eta_n^o P_n^* - R_n^*)}{\sum_{n=1}^{N} y_n^{(k)} P_n^*}$.
8: **goto** step (2).
9: **end**
10: Update $\mathbf{y}^{(k+1)} = \arg\max_{\mathbf{y}\in\mathcal{Y}} \min_{\mathbf{P},\mathbf{B}} U(\mathbf{y}, \eta(\mathbf{y}^{(k)}))$.
11: **If** $\eta(\mathbf{y}^{(k+1)}) - \eta(\mathbf{y}^{(k)}) < \epsilon_2$, **then**
12: Set $\eta^* = \eta(\mathbf{y}^{(k)})$.
13: **exit**.
14: **else**
15: Update $k = k + 1$.
16: **goto** step (2).
17: **end**

Then we can prove that $\eta(\mathbf{y}^{(k+1)}) \geq \eta(\mathbf{y}^{(k)})$ by following (4.50) and (4.51), and the fact that $U(\mathbf{y}, \alpha)$ decreases with α.

If the equality is achieved in (4.51), it means

$$U^* \triangleq \max_{\mathbf{y}\in\mathcal{Y}} \min_{\mathbf{P},\mathbf{B}} U(\mathbf{y}, \eta(\mathbf{y}^{(k)})) = 0.$$

This yields the global solution of $\eta^* = \eta(\mathbf{y}^{(k)})$ according to [41]. This ends the proof. □

According to Theorem 4.6, we can now develop an iterative algorithm to solve the problem, as summarized in Table 4.4.

As shown in step 2 of the algorithm, the objective function of the first subproblem can be written as

$$\max_{\mathbf{P},\mathbf{B}} \left\{ \sum_{n=1}^{N} y_n \left(\phi_n R_n - (\phi_n \eta_n^o - \alpha) P_n \right) \right\}. \tag{4.52}$$

We can easily prove that this objective function is jointly concave on $(\mathbf{P}, \mathbf{B})$. Therefore, we can utilize the classic convex optimization tools to solve it, such as the subgradient method and the interior point method.

https://doi.org/10.1017/9781108277389.005 Published online by Cambridge University Press

In step 10 of the algorithm, the second subproblem can be expressed as

$$\max_{\mathbf{y}\in\mathcal{Y}} \min_{\mathbf{P},\mathbf{B}} \sum_{n=1}^{N} y_n(\phi_n(\eta_n^o P_n - R_n) - \alpha P_n).$$

This problem is a bit difficult to solve. However, since a quasi-convex function attains its maximum on a vertex of a convex polyhedron [43], we can rewrite the objective function as

$$\min_{\mathbf{P},\mathbf{B}} \max_{n} \left\{\phi_n(\eta_n^o P_n - R_n) - \alpha P_n\right\}.$$

Moreover, according to the parametric optimization theory, we can further convert the problem into

$$\min_{\mathbf{P},\mathbf{B}} \tau,$$

subject to (4.44a)–(4.44d), and

$$\phi_n(\eta_n^o P_n - R_n) - \alpha P_n \leq \tau, \forall n.$$

Now the problem has been converted into a convex one, thus standard convex optimization methods can be utilized to effectively solve it.

4.4.3 Numerical Results

In this section, we will provide simulation results to show the performance of the proposed multi-objective energy-efficient algorithm. A multi-RAT HetNet consisting of two RATs is considered. The two networks have bandwidths of 1 MHz and 2 MHz, respectively. The channel model between the AP and users follows the i.i.d Rayleigh fading model. We assume that each uplink user has the same maximum transmit power of 1 W and the same data rate requirement of $R_{\min}$. Without loss of generality, the power amplifier efficiency is set as 100% for all users. Other major parameters are listed in Table 4.5 unless otherwise stated. We consider a simple symmetric scenario to validate the effectiveness of our proposal where the distances between each user and its access point are the same.

Table 4.5 System parameters

Parameters	Settings
Noise	-174 dBm/Hz
P^{I}	0.1 W
P_1^{D}, P_2^{D}	10 mW/MHz, 5 mW/MHz
W_1, W_2	2 MHz, 1 MHz
$P_n^{\max}, \forall n$	1 W
$\mathbf{\Delta}$	10^{-4}
ϵ_1, ϵ_2	10^{-4}, 0.1
$\omega_{m,n}, \forall m, n$	1
Γ_1, Γ_2	1
α_1, α_2	3, 4

https://doi.org/10.1017/9781108277389.005 Published online by Cambridge University Press

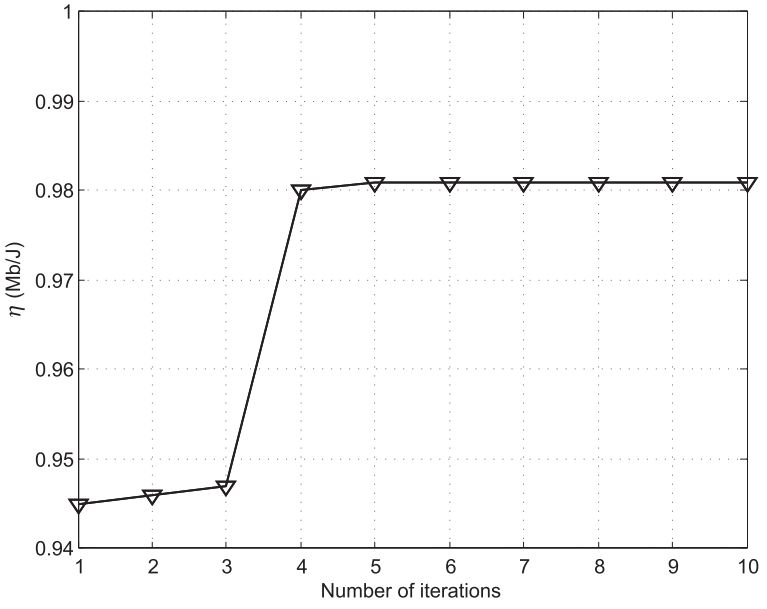

(a) The convergence of η.

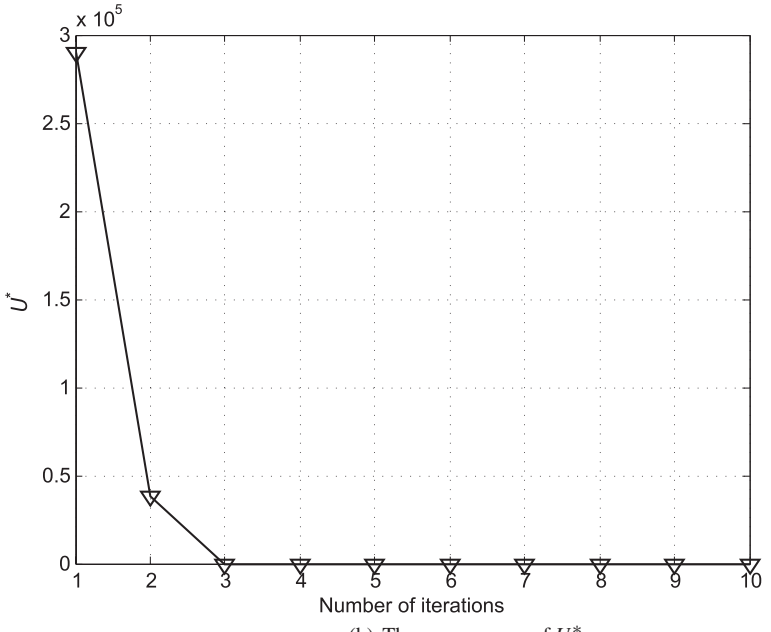

(b) The convergence of U^*.

Figure 4.14 The convergence speed of the proposed algorithm.

First, we examine the convergence rate of the proposed algorithm in Fig. 4.14. From the figure, $\eta(y^{(k)})$ converges to its maximum value while $U^{(k)}$ converges to 0 after only 4–6 iterations, which confirms our analysis. Moreover, since the first subproblem is a standard convex fractional programming problem, it converges fast. Therefore,

https://doi.org/10.1017/9781108277389.005 Published online by Cambridge University Press

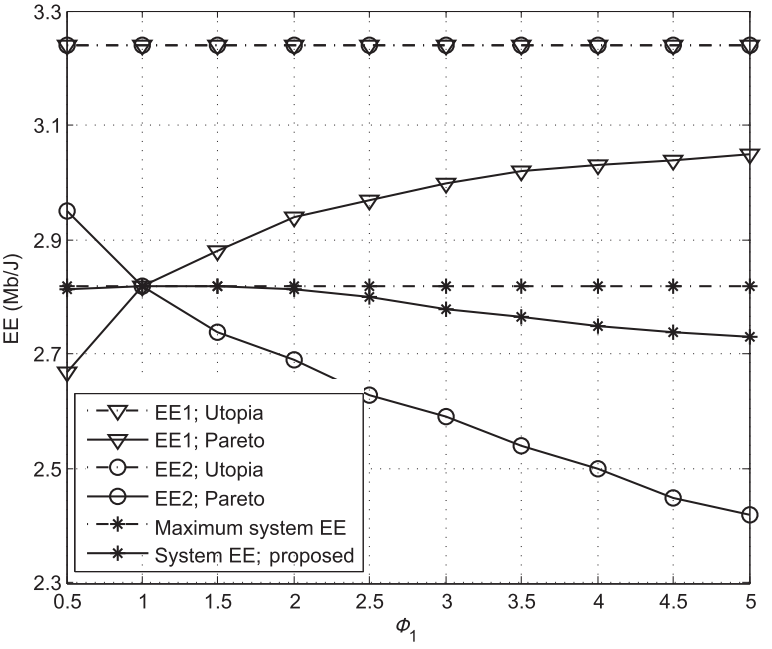

Figure 4.15 EE versus ϕ_1 in the symmetric scenario, $\phi_2 = 1$, $R_{\min} = 2$ Mbps. © 2015 IEEE. Reprinted, with permission, from Yu, G., 2015, 'Muilt-Objective Energy Efficient Resource Allocation for Multi-RAT Heterogeneous Networks', *IEEE Journal on Selected Areas in Communications*, vol. 33, no. 10, pp. 2118–2127.

the convergence speed of our proposed algorithm is fast and suitable for practical implementation.

Figure 4.15 shows the EE with different weights for user 1, ϕ_1, while the weight of user 2 is fixed to 1, i.e., $\phi_2 = 1$, and $R_{\min} = 2$Mbps. From the figure, the Utopia EE exactly serves as an upper bound of the EE for both users according to its definition. Moreover, with the increase of the weight, ϕ_1, the EE of user 1 increases gradually and finally reaches its maximum/Utopia EE. Meanwhile, the EE of user 2 decreases with ϕ_1, since more resource will be allocated to user 1 as its weight value increases, which demonstrates that an EE tradeoff between the two users can be achieved by the proposed algorithm. In the figure, we also compare the overall system EE of the proposed algorithm with the maximum overall system EE, which can be achieved by the classical Dinkelbach algorithm. The results in this figure show that, when $\phi_1 = \phi_2 = 1$, both users can achieve the same EE, which is also the maximum system EE. When the two weights are different, there exists a gap between the EE of our algorithm and the maximum system EE. Fortunately, this gap is rather small, which indicates that our algorithm can achieve a near-optimal EE performance.

We further test the EE performance with different user data rate requirements. In Fig. 4.16, the EE for users with different data rate requirements, $R_{\min}$, is depicted, where $\phi_1 : \phi_2 = 1 : 1$. The results in this figure show that the EE decreases with $R_{\min}$, which can be readily explained. When $R_{\min}$ is smaller, a larger EE can be achieved due to more freedom in the resource allocation algorithm. However, when $R_{\min}$ goes larger,

https://doi.org/10.1017/9781108277389.005 Published online by Cambridge University Press

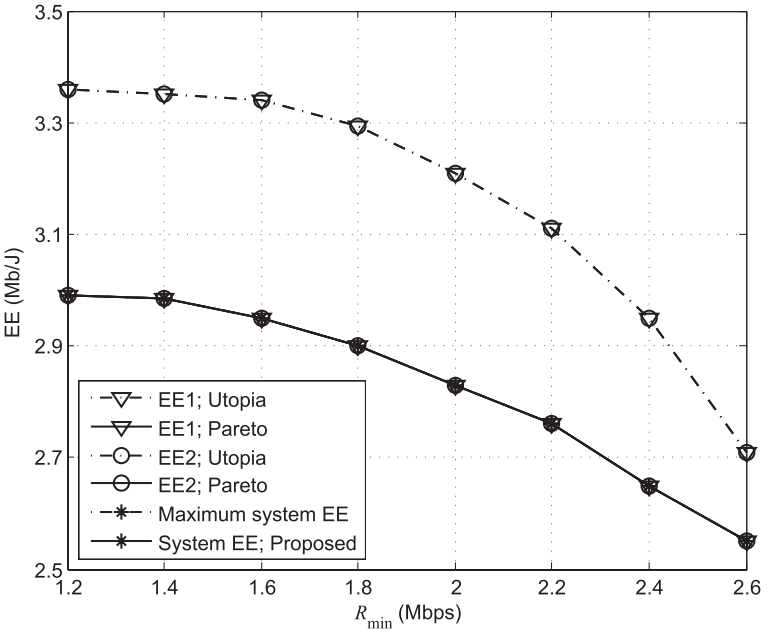

Figure 4.16 EE versus $R_{\min}$. $\phi_1 : \phi_2 = 1 : 1$. © 2015 IEEE. Reprinted, with permission, from Yu, G., 2015, 'Muilt-Objective Energy Efficient Resource Allocation for Multi-RAT Heterogeneous Networks', *IEEE Journal on Selected Areas in Communications*, vol. 33, no. 10, pp. 2118–2127.

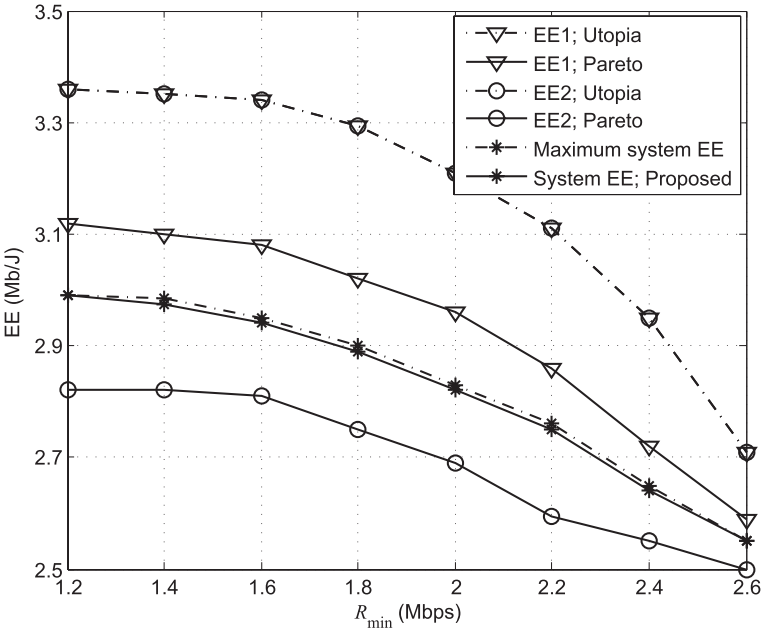

Figure 4.17 EE versus $R_{\min}$. $\phi_1 : \phi_2 = 2 : 1$. © 2015 IEEE. Reprinted, with permission, from Yu, G., 2015, 'Muilt-Objective Energy Efficient Resource Allocation for Multi-RAT Heterogeneous Networks', *IEEE Journal on Selected Areas in Communications*, vol. 33, no. 10, pp. 2118–2127.

https://doi.org/10.1017/9781108277389.005 Published online by Cambridge University Press

more resources will be allocated to increase the data rate, and in this case the EE will be inevitably decreased. We can also observe from the figure that the proposed algorithm can achieve the maximum system EE when $\phi_1 = \phi_2$, which is similar to the results in Fig. 4.15.

In Fig. 4.17, we further illustrate the results when $\phi_1 : \phi_2 = 2 : 1$. In this case, although both users can achieve the same Utopia EE, user 1 will achieve a larger EE than user 2 due to its relatively larger weight. We can also see from the results that the gap between Utopia EE and the Pareto-optimal EE for user 2 is almost twice larger than that of user 1. This is resulting from the weighted Tchebycheff algorithm, which minimizes the maximum gap between Utopia and Pareto-optimal EEs. Furthermore, in the case of $\phi_1 : \phi_2 = 2 : 1$, our algorithm cannot achieve maximum system EE, as has been explained previously.

References

[1] Z. Niu, "TANGO: Traffic-aware network planning and green operation," *IEEE Wireless Commun.*, vol. 18, no. 5, pp. 25–29, Oct. 2011.

[2] J. Wu, S. Zhou, and Z. Niu, "Traffic-aware BS sleeping control and power matching for energy-delay tradeoffs in green cellular networks," *IEEE Trans. Wireless Commun.*, vol. 12, no. 8, pp. 4196–4209, Aug. 2013.

[3] E. Oh, B. Krishnamachari, X. Liu, and Z. Niu, "Toward dynamic energy-efficient operation of cellular network infrastructure," *IEEE Commun. Mag.*, vol. 49, no. 6, pp. 56–61, Jun. 2011.

[4] Z. Niu, Y. Wu, J. Gong, and Z. Yang, "Cell zooming for cost-efficient green cellular networks," *IEEE Commun. Mag.*, vol. 48, no. 11, pp. 74–79, Nov. 2011.

[5] D. Feng, L. Lu, Y. Wu, G. Li, and S. Li, "Device-to-device communications underlaying cellular networks," *IEEE Trans. Commun.*, vol. 61, no. 8, pp. 3541–3551, Aug. 2013.

[6] G. Yu, L. Xu, D. Feng et al., "Joint mode selection and resource allocation for device-to-device communications," *IEEE Trans. Commun.*, vol. 62, no. 11, pp. 3814–3824, Nov. 2014.

[7] J. Liu, T. Zhao, S. Zhou, Y. Cheng, and Z. Niu, "CONCERT: A cloud-based architecture for next-generation cellular systems," *IEEE Wireless Commun.*, vol. 21, no. 6, pp. 14–22, Dec. 2014.

[8] S. Zhou, T. Zhao, Z. Niu, and S. Zhou, "Software-defined hyper-cellular architecture for green and elastic wireless access ," *IEEE Commun. Mag.*, vol. 54, no. 1, pp. 12–19, Jan. 2016.

[9] C. Xiong, G. Y. Li, S. Zhang, Y. Chen, and S. Xu, "Energy- and spectral-efficiency tradeoff in downlink OFDMA networks," *IEEE Trans. Wireless Commun.*, vol. 10, no. 11, pp. 3874–3886, Nov. 2011.

[10] D. W. K. Ng, E. S. Lo, and R. Schober, "Energy-efficient resource allocation in multi-cell OFDMA systems with limited backhaul capacity," *IEEE Trans. Wireless Commun.*, vol. 11, no. 10, pp. 3618–3631, Oct. 2012.

[11] C. Xiong, G. Y. Li, S. Zhang, Y. Chen, and S. Xu, "Energy-efficient resource allocation in OFDMA networks," *IEEE Trans. Commun.*, vol. 60, no. 12, pp. 3767–3778, Dec. 2012.

[12] G. Miao, N. Himayat. G. Y. Li, and S. Talwar, "Low-complexity energy-efficient scheduling for uplink OFDMA," *IEEE Trans. Commun.*, vol. 60, no. 1, pp. 112–120, Jan. 2012.

[13] O. Onireti, F. Heliot, and M. A. Imran, "On the energy efficiency-spectral efficiency trade-off in the uplink of CoMP system," *IEEE Trans. Wireless Commun.*, vol. 11, no. 2, pp. 556–561, Dec. 2012.

[14] G. Miao, "Energy-efficient uplink multi-user MIMO," *IEEE Trans. Wireless Commun.*, vol. 12, no. 5, pp. 2302–2313, May 2013.

[15] S. Buzzi, G. Colavolpe, D. Saturnino, and A. Zappone, "Potential games for energy-efficient power control and subcarrier allocation in uplink multicell OFDMA systems," *IEEE J. Sel. Topics Signal Process.*, vol. 6, no. 2, pp. 89–103, Nov. 2012.

[16] Z. Shen, A. Khoryaev, E. Eriksson et al., "Dynamic uplink-downlink configuration and interference management in TD-LTE," *IEEE Commun. Mag.*, vol. 50, no. 11, pp. 51–59, Nov. 2012.

[17] R. Ratasuk, A. Ghosh, W. Xiao, et al., "TDD design for UMTS long-term evolution," in *Proc. IEEE PIMRC 2008*, Cannes, France, pp. 1–5, Sept. 2008.

[18] 3GPP TS 36.828, "Evolved universal terrestrial radio access (E-UTRA); Further enhancements to LTE time division duplex (TDD) for downlink-uplink (DL-UL) interference management and traffic adaptation (Release 11)."

[19] H. Holma, S. Hekkinen, O. A. Lehtinen, and A. Toskala, "Interference considerations for the time division duplix node of the UMTS terrestrial radio access," *IEEE J. Sel. Areas Commun.*, vol. 18, no. 8, pp. 1386–1393, Aug. 2000.

[20] S. Boyd and L. Vandenberghe, *Convex Optimization*, Cambridge University Press, 2004.

[21] Y.-C. Jong, "An efficient global optimization algorithm for nonlinear sum-of-ratios problem," May 2012. www.optimization-online.org/DB_FILE/2012/08/3586.pdf.

[22] S. Boyd, L. Xiao, and A. Mutapcic, "Subgradient methods," lecture notes, EE392o: Optimization Projects, Stanford University, Autumn Quarter 2003–2004.

[23] "MSA: A key technology for the evolution of future wireless networks," Huawei Whitepaper, Jun 2013. www.huawei.com/mediafiles/CORPORATE/PDF/Magazine/communicate/70/HW_267909.pdf.

[24] I. F. Akyildiz, D. M. Gutierrez-Estevez, R. Balakrishnan, and E. Chavarria-Reyes, "LTE-Advanced and the evolution to Beyond 4G (B4G) systems," *Physical Commun.*, vol. 10, no. 1, pp. 31–60, Mar. 2014.

[25] C. Kim, R. Ford, and S. Rangan, "Joint interference and user association optimization in cellular wireless networks," in *Proc. IEEE Asilomar Conf. on Signals, Systems and Computers*, Pacific Grove, CA, Nov. 2014, pp. 511–515.

[26] Q. Ye, B. Rong, Y. Chen et al., "User association for load balancing in heterogeneous cellular networks," *IEEE Trans. Wireless Commun.*, vol. 12, no. 6, pp. 2706–2716, Jun. 2013.

[27] A. Damnjanovic, J. Montojo, Y. Wei, et. al, "A survey on 3GPP heterogeneous networks," *IEEE Wireless Commun.*, vol. 18, no. 3, pp. 10–21, Jun. 2011.

[28] S. S. Yong, T. Q. S. Quek, M. Kountouris, and H. Shin, "Energy efficient heterogeneous cellular network," *IEEE J. Sel. Areas Commun.*, vol. 31, no. 5, pp. 840–850, May 2013.

[29] S. Navaratnarajah, A. Saeed, M. Dianati, and M. A. Imran, "Energy efficiency in heterogeneous wireless access networks," *IEEE Wireless Commun.*, vol. 20, no. 5, pp. 37–43, Oct. 2013.

[30] Y. Choi, H. Kim, S. Han, and Y. Han, "Joint resource allocation for parallel multi-radio access in heterogeneous wireless retworks," *IEEE Trans. Wireless Commun.*, vol. 9, no. 11, pp. 3324–3329, Nov. 2010.

[31] S. Singh, H. S. Dhillon, and J. G. Andrews, "Offloading in heterogeneous networks: Modeling, analysis and design insights," *IEEE Trans. Wireless Commun.*, vol. 12, no. 5, pp. 2484–2497, May 2013.

[32] D. Cao, S. Zhou, and Z. Niu, "Improving the energy efficiency of two-tier heterogeneous cellular networks through partial spectrum reuse," *IEEE Trans. Wireless Commun.*, vol. 12, no. 8, pp. 4129–4141, Aug. 2013.

[33] D. Cao, S. Zhou, and Z. Niu, "Optimal combination of BS densities for energy-efficient two-tier heterogeneous cellular networks," *IEEE Trans. Wireless Commun.*, vol. 12, no. 9, pp. 4350–4362, Sept. 2013.

[34] S. He, Y. Huang, H. Wang, S. Jin, and L. Yang, "Leakage-aware energy-efficient beamforming for heterogeneous multicell multiuser systems," *IEEE J. Sel. Areas Commun.*, vol. 32, no. 6, pp. 1268–1281, Jul. 2014.

[35] Z. Xu, C. Yang, G. Y. Li, Y. Liu, and S. Xu, "Energy-efficient CoMP precoding in heterogeneous networks," *IEEE Trans. Signal Process.*, vol. 62, no. 4, pp. 1005–1017, Feb. 2014.

[36] Y. Huang, X. Zhang, J. Zhang et al., "Energy efficient design in heterogeneous cellular networks based on large-scale user behavior constraints," *IEEE Trans. Wireless Commun.*, vol. 13, no. 9, pp. 4746–4757, Sept. 2014.

[37] X. Ma, M. Sheng, and Y. Zhang, "Green communications with network cooperation: A concurrent transmission approach," *IEEE Commun. Lett.*, vol. 16, no. 12, pp. 1952–1955, Dec. 2012.

[38] G. Lim and L. J. Cimini, "Energy-efficient cooperative relaying in heterogeneous radio access networks," *IEEE Wireless Commun. Lett.*, vol. 1, no. 5, pp. 476–479, Oct. 2012.

[39] G. Lim, C. Xiong, L. J. Cimini, and G. Y. Li, "Energy-efficient resource allocation for OFDMA-based multi-RAT networks," *IEEE Trans. Wireless Commun.* vol. 13, no. 5, pp. 2696–2705, May 2014.

[40] R. T. Marler and J. S. Arora, "Survey of multi-objective optimization methods for engineering," *Struct. Multidiscip. O.*, vol. 26, no. 6, pp. 369–395, Apr. 2004.

[41] A. I. Barros, J. B. G. Frenk, S. Schaible, and S. Zhang, "A new algorithm for generalized fractional programs," *Math. Program.*, vol. 72, no. 2, pp. 147–175, Feb. 1996.

[42] J. P. Crouzeix and J. A. Ferland, "Algorithms for generalized fractional programming," *Math. Program.*, vol. 52, no. 2, pp. 191–207, Oct. 1991.

[43] M. Avriel, W. E. Diewert, S. Schaible, and I. Zang. "Generalized concavity," *Mathematical Concepts and Methods in Science and Engineering*, vol. 36, Plenum Press, 1988.

[44] M. Sion, "On general minimax theorems," *Pacific J. Math.*, vol. 8, no. 1, pp. 171–176, Mar. 1958.

[45] W. Dinkelbach, "On nonlinear fractional programming," *Manage. Sci.*, vol. 13, pp. 492–498, Mar. 1967.